Process Safety and Environmental Protection 178 (2023) 396–413

Contents lists available at ScienceDirect

Process Safety and Environmental Protection

journal homepage: www.journals.elsevier.com/process-safety-and-environmental-protection

Exergy-based techno-economic and environmental assessments of a proposed integrated solar powered electricity generation system along with novel prioritization method and performance indices

Aslı Tiktaş [a], Huseyin Gunerhan [b], Arif Hepbasli [c,*], Emin Açıkkalp [d]

[a] Department of Mechanical Engineering, Faculty of Engineering and Architecture, Kırşehir Ahievran University, 40100 Bağbaşı, Kırşehir, Turkey
[b] Department of Mechanical Engineering, Faculty of Engineering, Ege University, 35100 Bornova, Izmir, Turkey
[c] Department of Energy Systems Engineering, Faculty of Engineering, Yasar University, 35100 Bornova, Izmir, Turkey
[d] Department of Mechanical Engineering, Faculty of Engineering, Eskisehir Technical University, 26555 Eskisehir, Turkey

ARTICLE INFO

Keywords:
Organic Rankine cycle
Absorptional heat transformer
Solar energy
Advanced exergy analysis
Advanced exergoeconomic analysis
Optimization

ABSTRACT

This study focused on the two important gaps in the literature. The first is solar energy- powered electricity generation in a more economical way via the integration of flat plate solar collector (FPSC), an Organic Rankine Cycle (ORC), and an absorptional heat transformer (AHT) system. Another gap is advanced exergy analysis of the AHT cycle/ORC process based on renewable energy integration to reveal clues for improving the system. To close these gaps, a novel system including a lithium bromide AHT cycle-ORC with a FPSC system application was proposed in this study. In this proposed system, the temperature of the heat source for the ORC system was upgraded via an integration of the AHT and FPSC cycles. The main components of the AHT cycle are the condenser (ABScon), refrigerant cycle pump (P1), evaporator (EV), absorber (ABS), solution heat exchanger (SHX), absorbent cycle pump (P2), expansion valve (V), generator (Gen), ORC turbine (ORCT) and ORC condenser (ORCcon). To demonstrate the electricity production from solar energy in a more economical way thanks to the proposed system, a comparison was made with similar-scaled existing solar power plants. The results supported the main purpose of this study. The annual electricity production with the proposed system was calculated as 2601 MWh, with initial investment cost and payback period values of US$3.924 million and 4.531 years, respectively. The conventional and advanced exergy, exergoeconomic, environmental impact, and sustainability analyzes were also performed. Based on these, the novel performance parameters and prioritization method were proposed to assess the improvement potential of the system. The results indicated that SHX and FPSC had the highest exergy destruction rates (EDRs) of 23.711% and 21.849% over 5853.89 kW due to the stronger thermal and chemical reactions. Similarly, Gen, FPSC, and SHX had the highest ED cost rates (CRs) of 67.59%, 59.09%, and, 47.98%, respectively. Gen, V, and ORCcon were higher contributors to the exergy destruction rates of almost all the components. However, these showed an adverse manner for irreversibility activities. So, the temperatures of Gen and ORCcon should be optimized carefully. ABScon, P2, P1, ABS, Gen, ORCT, and ORCcon had high development priority to improve the whole system.

1. Introduction

Following a recent statistical report, the global primary energy demand in 2021 increased by 5.8% compared to the previous year and exceeded its pre-pandemic value by 1.3% (bp, 2022). The data from this statistical report indicated that the global energy consumption this year was 3 points above the average annual increase over the 2000–2019 period. Such a rapid surge in energy demand and consumption triggered significant global-scaled problems i.e., energy crisis and distortion of green and sustainable environment. Hence, the integration of renewable energy sources with effective waste heat recovery mechanisms is an

Abbreviations: ABS, Absorber; ABScon, Absorption heat transformer condenser; EV, Evaporator; Gen, Generator; ORC, Organic Rankine cycle; ORCcon, ORC condenser; ORCT, ORC turbine; P1, Pump 1 (or refrigerant cycle pump); P2, Pump 2 (or absorbent cycle pump); SHX, Solution heat exchanger; V, Expansion valve.

* Corresponding author.
E-mail addresses: aslitiktas6@hotmail.com, asli.tiktas@ahievran.edu.tr (A. Tiktaş), huseyin.gunerhan@ege.edu.tr (H. Gunerhan), arifhepbasli@gmail.com, arif.hepbasli@yasar.edu.tr (A. Hepbasli), eacikkalp@gmail.com (E. Açıkkalp).

https://doi.org/10.1016/j.psep.2023.08.048
Received 7 June 2023; Received in revised form 25 July 2023; Accepted 16 August 2023
Available online 19 August 2023

Nomenclature

adp.GWP	Global warming potential of substance with the atmospheric degradation.
AEC	Annual energy consumption (kWh/year).
ALR	Annual leakage rate (kg/years).
b	Chemical exergy value per mole (kW/mol).
c	Cost associated with exergy streams ($/kWh).
C	Substance charge mass causing emission (kg).
$\dot{C}$	Annualized cost rate ($/h).
CECPI	Chemical economic plant cost index.
CRF	Capital recovery factor.
EcoEF	Ecological effect factor.
EEF	Environmental effect factor.
EF	Emission factor of plant.
Em	CO_2 emission*(kg)*.
EOL	End of life substance (years).
ExSI	Exergetic sustainability index.
f	Exergoeconomic factor.
FExWR	Fuel exergy waste ratio.
GWP	Global warming potential.
h	Specific enthalpy (kJ/kg).
i	Interest rate.
L	Life time (years).
$\dot{m}$	Mass flow rate (kg/s).
mr	Recycled material mass (kg).
M	Price index.
MM	Equivalent CO_2emission pertained with the production of material mass (kg).
n	Entire number of component.
N	Entire operating period (years).
RDF	Substance disposal emissions (kg).
RM	Equivalent CO_2emission pertained with the recycled material mass (kg).
RMF	Substance manufacturing emissions (kg).
s	Specific entropy (kJ/kg.K).
S	Size.
SEF	Social ecological factor.
t	Time (s).
T	Temperature (°C or K).
x	LiBr concentration (wt%).
z	Mole fraction.

Subscripts

0	Dead-state.
1	Inlet.
2	Outlet.
b	Base.
c	Component.
D	Destruction.
eq.mfg	Equipment manufacturing.
eq.rcy	Equipment recycling.
F	Fuel.
i	Relevant stream.
k	Equipment.
m	Material.
mexo	Mexogenous.
mod	Modified.
P	Product.
r	Contributed component.
re.mfg	Substance manufacturing emissions.
T	Total.

Superscripts

AV	Avoidable.
Ch	Chemical.
EN	Endogeneous.
EX	Exogenous.
Ph	Physical.
UN	Unavoidable.

Greek letters

ϕ_k	Maintenance factor.
η	Efficiency.

intelligent and sustainable solution to meeting the rising energy demand. In this context, the implementation of these applications has great importance for the industry, which is one of the sectors with the highest energy consumption. However, most of the industrial processes involve high temperature or power requirements and almost half of the energy consumed is thrown into the environment in the form of low-grade waste heat. Organic Rankine Cycle (ORC) systems create a strong potential to meet the high-power requirement in the industry together with the sustainable energy concept. Because the prominent features of ORC systems are flexible structure, simplest infrastructure and installation, easiest integration to the renewable energy source, lowest capital cost, and power generation with medium-grade heat sources. For the mentioned reasons, the most practical and economical way to produce electricity from low- grade waste heat is seen as the utilization of the ORC system (Quoilin et al., 2013). Providing multigeneration outputs by integrating ORC systems with novel prime movers and complex waste heat recovery mechanisms has attracted much more attention in recent years (Tiktas et al., 2022; Javed and Tiwari, 2023; Bagherzadeh et al., 2020; Yağlı et al., 2021; Wang et al., 2021). Among the integrable renewable energy sources to the ORC system, solar energy comes to the fore due to its easy integration into most processes with abundant and cleaner features. However, the practical implementation of low-cost solar energy systems, such as flat plate solar collectors (FPSCs), provides low-grade heat to the ORC system, and with this heat grade, the ORC system cannot work. For this reason, parabolic through or Fresnel solar collectors are generally used in existing solar power plants for electricity generation with solar energy support. In this case, the cost of solar collectors constitutes an important portion of the total initial investment cost of the system and also requires additional maintenance costs to be covered. Therefore, there is a significant gap in the literature due to the constraint on generating electricity more economically by integrating FPSCs with the ORC system. To close this gap, the current study, which includes the integration of these two advantageous systems with each other by utilization of absorption technology, was performed. In addition, the advanced exergy analysis of the absorptional heat transformer (AHT) cycle/ORC process based on renewable energy integration with this study, besides closing another important gap in the literature, reveals the clues for the improvement of such a system.

In general, AHT is one of the most important technologies in the 21st century for energy recovery and/or temperature-raising applications (Horuz and Kurt, 2010; Donnellan et al., 2014; Ma et al., 2021). With this technology, high-grade energy output in the absorber is obtained as a result of absorption processes from the low-grade waste heat sent to the generator (Wakim and Rivera-Tinoco, 2019). The environmental friendliness and excellent energy recovery features of AHT explain the intense interest of researchers in this technology. Liu et al (Liu et al., 2017). estimated optimal design conditions for the combination of single-stage AHT system and solar energy source by implementing the ratio method. They observed 1318 kWh of heat output per day for these conditions. Yari et al (Yari et al., 2017). improved the maximum

temperature enhancement by 18%– 27% via the utilization of double-stage AHT system. With the double AHT system developed by Wang et al (Wang et al., 2018a). for the carbon dioxide capturing process, the total production cost decreased by 10.7 $/t-$CO_2$, and the exergy efficiency of the system increased by 1.85%. Mosaffa and Garousi (Mosaffa and Farshi, 2020) utilized a double-effect AHT system for the carbon dioxide power cycle to enhance the exergy efficiency of the system by preheating carbon dioxide before entering the generator.

In the literature, the idea of generating electricity by raising the temperature of the heat source in the ORC system with AHT supplementation was first introduced by Chaiyat (Chaiyat, 2014). In this study, to generate 20 kW of electricity from an ORC system, a 250 kW AHT system was utilized with a rising final temperature of 90–110℃. From economic evaluations, the electricity cost of Thailand and the payback period were estimated yearly US$5945.82 and 15.96 years, respectively. In this respect, this integration has been convenient and costly in terms of energy efficiency due to the relatively higher AHT system cost per produced electricity power. This situation caused the researchers not to dwell on this subject sufficiently and the absorption effect was mostly tested on cooling systems. Especially, lithium bromide-water solution absorption cooling systems (LiBr-water cycle) have attracted increasing attention in obtaining cooling load by using low-grade heat input due to their environmentally friendly properties (Nikbakhti et al., 2020) when the temperature of the heat source is $100^{\circ}C$-$175^{\circ}C$, this cooling system shows a better thermodynamic performance compared to the Kalina cycle (Wang et al., 2018b). Research on the LiBr-water cycle and integration of ORC systems is relatively mature. In recent years, new complex energy recovery processes by combining different subsystems have received considerable attention. The integrated system presented by Razmi et al (Razmi et al., 2019)., which included ORC, compressed air energy storage, and absorption cooling systems, produced 2280 kW of electrical energy rate and 416.7 kW of cooling load. This system had 13, 15% higher efficiency compared to the system, in which only compressed air energy was used. Alsagri et al (Alsagri et al., 2019). integrated the ORC and the subcooled compressed air energy storage systems. With this design, they managed to generate approximately 20% more power than the ORC system. In another study (Emadi et al., 2020), a double loop was integrated and developed by combining solid oxide fuel cell, ORC, and LiBr-water cycle systems. This waste heat recycling system was able to supply 20.7% of the electricity while at the same time providing a cooling load of 567 kW.

The LiBr-water cycle is generally used for the better thermodynamic performance of other integrated subsystems or the higher cooling load. For example, when the temperature of the environment where the cooling load is obtained was $2^{\circ}C - 10^{\circ}C$. Yang et al (Yang et al., 2019). integrated a transcritical carbon dioxide process with the LiBr-water cycle and obtained a cooling load ranging from 36.08 kW to 39.68 kW. An increase in the cooling capacity of the system was made by 45% by combining the LiBr-water cycle and the Kalina cycle (Liu et al., 2020). A lithium chloride liquid dehumidification system was integrated with the LiBr-water cycle and based on the calculations, the maximum coefficient of performance for the system was 0.603 (Xu et al., 2021). These studies in the literature have shown that the cooling load capacity is significantly increased by integrating the LiBr-water cycle with other subsystems. In addition, studies are proving that the output pressure of the ORC turbine can be increased by reducing the output pressure in this way (Mohammadi et al., 2017; Azizi et al., 2023). For example, an attempt was made towards increasing the efficiency of the ORC system by using an absorption cooling system (Navongxay and Chaiyat, 2019). In this system design, the absorption unit replaced the condenser of the ORC system, with energy and exergy efficiencies of 20.61% and 21.54%, respectively, and the system exhibited a better thermodynamic performance compared to the case where no improvement was made.

The solar energy integration of LiBr-water and ORC cycles is widely used in practice due to the need for a low-grade waste heat source in this application (Karabuga et al., 2023; Li et al., 2023). However, in this integration, mostly concentrated solar power technology (CSP) is preferred due to its high energy efficiency with the provision of sustainable solutions (Chuquin-Vasco et al., 2023; Pop et al., 2023). The National Renewable Energy Laboratory (NREL) database shows that in CSP technology, parabolic trough collectors are the most used collector group with a share greater than 80% among all installations ($author1$ et al., 32] </id><collab>NREL</collab>). Another strong alternative solar collector for the integration of solar energy and LiBr-water and ORC cycles is Fresnel solar collectors as a low-grade heat source (Sigue et al., 2023; Machado et al., 2023; Díaz Carrillo, 2023; Kumar, 2023).

As a result of the extensive literature research, it has been determined that solar energy- supported electricity generation with the ORC system is mainly carried out with high-cost CSP technologies. This is due to the technical constraint in integrating low-cost FPSC technology in electricity generation in this way. In this study, we propose to overcome this technical limitation through the integration of FPSC, ORC, and AHT.

Another important finding obtained from the literature research is that the researchers did not pay enough attention to this integrated system and instead focused heavily on ORC and absorption cooling systems, concerning the economic results of the study of Chaiyat (Chaiyat, 2014) based on the integration of ORC and AHT systems for electricity generation. Thus, there has been a tendency in the literature to use the absorption effect mostly on cooling systems. This highlights another important gap in the literature on electricity generation, with two powerful technologies, such as ORC and AHT, which are efficient as well as economically applicable at a practical level.

With the current study, the integration of FPSC application with ORC and AHT systems has been suggested to close these gaps in the literature and to provide electricity production more economically with powerful technologies.

The present study has focused on the two main gaps in the literature above. In this context, a lithium bromide AHT cycle-ORC system process assisted with an FPSC system application for electricity generation was proposed and evaluated exergetically. In this proposed system, it is also aimed to indicate how electricity production can be realized more economically with the integration of AHT, FPSC, and ORC systems, unlike existing small-medium-sized solar power plants. For this purpose, the techno-economic data obtained from the proposed system was compared with other solar power plants of similar capacities in the world. For this, the proposed system was modeled in Engineering Equation Solver (EES) and Transient System Simulation Software (TRNSYS) packages for an illustrative example of the city of Izmir, Turkey. The advanced exergy, exergo-economic, environmental impact, and sustainability analyses were implemented in this novel system. In this way, a rational way was proposed to integrate two powerful technologies of the 21st century, which was not emphasized much in the literature due to the negativities in economic parameters. With advanced exergy analysis, important clues were tried to be given for the development of this proposed system while novel performance indices were derived based on this analysis. For example, with the upgrade potential index (*UPI*) included in the derived novel indices, the feasible improvement potential contributions of each component in improving the overall performance of the system are expressed. Essentially, *UPI* combines other developed novel indices based on the advanced exergy analysis to realize the induced mechanism of ineffectiveness for each piece of equipment. Thus, unlike the performance indices available in the literature, it was suggested which equipment should be prioritized in improving the overall performance of the system with these indices, together with a numerical value. In addition, based on the novel indices derived here, the novel prioritization method with a three-stage rating system was proposed in detail for the improvement potential of the overall system. With this novel method, not only the improvement potentials of the equipment were graded, but also what kind of improvement model should be used for each of them was also specified.

2. System description and modelling

2.1. System description

The proposed system for electricity generation based on the AHT cycle-ORC system process assisted with low-grade solar energy application is shown in Fig. 1. In this system, for the ORC system component various ORC working fluid candidates, namely toluene, isopentane, R600, R123 and R245fa, were evaluated. However, for the AHT system, the LiBr-H_2O solution was utilized. With this proposed system, 1000 kW of mechanical power production from the ORC turbine was aimed. In this configuration, the required heat to operate the generator and evaporator in the AHT cycle was provided from a low-grade solar energy source application. In this regard, to reduce system costs and create low-grade waste heat, the required heat was obtained from flat FPSCs reaching a temperature of 80℃. Hence, the generator and evaporator temperature values were taken as 80℃. The absorber, absorption system condenser, and ORC turbine inlet temperatures were chosen as 150℃, 40℃, and 145 ℃, respectively, with a parametric study following the system flow to satisfy more than 17–19% of ORC system efficiency. With this approximation, it is aimed to exceed the thermal efficiency of the conventional PV system and constitute a comparable solar power plant such as the Saguaro ORC plant. In current small-medium scaled solar power plants using parabolic or Fresnel solar collector technologies, electricity generation takes place at a relatively high cost. Thus, unlike the existing solar power plants, it is aimed to produce more electricity more economically with the integration of FPSC and ORC cycle.

2.2. Process description

The water in the solution of the generator is evaporated and sent to the condenser at state 2. A fully saturated liquid form is obtained in the condenser at state 3 and is pumped to the evaporator at state 4. After evaporation takes place in the high-pressure region of the evaporator, it is sent to the absorber at state 5. The mixture, which is rich in LiBr, is produced in the generator and directed to the solution pump at state 8, and from there, it is pumped to the absorber at state 9. The mixture at the absorber is mixed with the steam from the evaporator at state 6. This mixture is returned from the absorber to the generator through the throttling valve at state 7. The waste heat in the absorber is used as heat input to the ORC system. The ORC working fluid enters the ORC turbine at state 10 while at state 11, it exits the turbine and enters the condenser. The mechanical work is produced through the expansion work performed in the ORC turbine. At state 12, the ORC working fluid is fully saturated in liquid form because of condensing process. Then, it is transmitted to the absorber for completion of the ORC cycle.

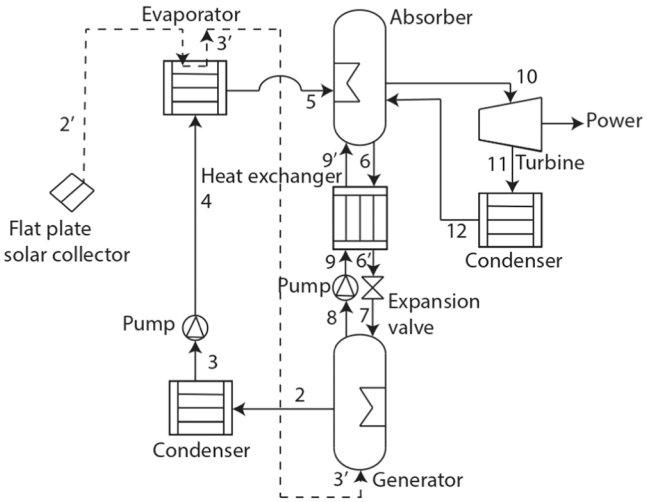

Fig. 1. Schematic description of the proposed system.

2.3. Flowsheet simulation

Table 1 indicates the flowsheet simulation results. The proposed system was modelled using the EES package. For the evaluation of this system, the selected special design parameters and assumptions made are summarized in Table 2 while the general assumptions are listed below:

a) Kinetic and potential energy changes are neglected.
b) Operation of the system occurs steadily.
c) The heat losses of the component to the environment are neglected.
d) The change of the voltage for all the components is neglected except for the pumps and valves.

3. Analyses

3.1. Energy analysis

To implement energy analysis based on the first law of thermodynamics in the proposed system, the mass and energy balance equations were utilized for each component. These equations are summarized in Table 3. For the five different ORC working fluids, the overall system energy efficiency values are compared in Fig. 2 to determine the best ORC working fluid from the energetic view. According to this figure, toluene, R123, and R600 demonstrated better energetic performances compared with others. Table 4 shows the energy analysis results for the best ORC working fluid.

3.2. Exergy analyses

The quality of energy based on the second law of thermodynamics was evaluated by performing an exergy analysis on the proposed system. In this way, the real work output of the system including the real conditions was compared to the ideal feasible work output involving the ideal conditions. Hence, it was possible to comment on the improvement potential of the system. In this regard, conventional and advanced exergy analyses were performed. In this study, the physical and chemical exergy rates were considered. The physical and chemical portions of exergy rates were defined with Eqs. (1–3) in the formulae section, respectively (Tiktas et al., 2022).

3.2.1. Conventional exergy analysis

In conventional exergy analysis, exergy fuel, product and destruction rates, and exergy efficiency were determined for each component along with the overall system. For this analysis, the exergy balance equations based on the second law of thermodynamics were utilized for each system component. These equations are given in Table 5.

Table 1
Flowsheet simulation results.

Stream	$P[kPa]$	$T[℃]$	$\dot{m}$ $[kg/s]$	$h[kJ/kg]$	$s\left[\frac{kJ}{kgK}\right]$	$X(\%)$
0	3.169	25	2.155	104.8	0.367	
1	3.169	90	2.155	2669	8.928	
2	7.381	80	2.155	2649	8.483	
3	7.381	40	2.155	167.5	0.5723	
4	47.37	80	2.155	334.9	1.075	
5	47.37	80	2.155	2643	7.611	
6	47.37	150	43.42	349.7	0.7354	66.77
7	80.95	156.6	43.42	349.7	0.8015	63.46
8	47.37	150	41.27	349.7	0.7354	66.77
9	41.48	145	41.27	340.9	0.7139	66.77
10	1926	145	18.87	463.9	1.71	
11	75.71	20	18.87	410.9	1.719	
12	75.71	20	18.87	221	1.074	

Table 2
Design parameter and assumption specification of the proposed system.

Design parameters		Assumptions	
Absorptional heat transformer system	*ORC system*	*Absorptional heat transformer system*	*ORC system*
Generator temperature:80℃ Condenser temperature:40℃ Evaporator temperature:80℃ Absorber temperature:150℃ Solution heat exchanger temperature:145℃ Refrigerant-absorbent mixture: LiBr-water solution	ORC working fluid: R123 Evaporator temperature:145℃ Condenser temperature:20℃ Turbine isentropic efficiency: 0.95 Output power of turbine: 1 MW	The water leaving the condenser is in the saturated liquid phase. The water leaving the evaporator is in the saturated vapor phase. The LiBr-water mixture separated from the absorber is in equilibrium at the absorber pressure and temperature. The LiBr-water mixture leaving the generator is in equilibrium at the absorber pressure and temperature. The temperature of water leaving the generator is at the generator temperature.	The organic working fluid is saturated vapor at the turbine inlet. At the condenser outlet, the organic working fluid is in saturated liquid state.

Table 3
Mass and energy balance equations.

Equipment	Mass balance equation	Energy balance equation
Gen	$\dot{m}_7 = \dot{m}_2 + \dot{m}_8$ $\dot{m}_7 X_7 = \dot{m}_8 X_8$ $f = X_7/(X_8 - X_7)$	$\dot{Q}_{gen} = \dot{m}_2[f h_8 + h_2 - (f+1)h_7]$
ABScon	$\dot{m}_2 = \dot{m}_3$	$\dot{Q}_{con} = \dot{m}_2(h_2 - h_3)$
P1	$\dot{m}_3 = \dot{m}_4$	$\dot{m}_3 h_3 + \dot{W}_p = \dot{m}_4 h_4$
EV	$\dot{m}_4 = \dot{m}_5$	$\dot{Q}_{ev} = \dot{m}_2(h_5 - h_4)$
ABS	$\dot{m}_5 + \dot{m}_{9'} = \dot{m}_6$ $\dot{m}_6 X_6 = \dot{m}_{9'} X_{9'}$	$\dot{Q}_{abs} = \dot{m}_2[h_5 + f h_9 - (f+1)h_6]$
SHX	$\dot{m}_6 = \dot{m}_{6'}$ $\dot{m}_9 = \dot{m}_{9'}$ $\dot{m}_6 X_6 = \dot{m}_{6'} X_{6'}$ $\dot{m}_9 X_9 = \dot{m}_{9'} X_{9'}$	$\dot{m}_6 h_6 + \dot{m}_9 h_9 = \dot{m}_{6'} h_{6'} + \dot{m}_{9'} h_{9'}$
P2	$\dot{m}_8 = \dot{m}_9$	$\dot{m}_8 h_8 + \dot{W}_p = \dot{m}_9 h_9$
V	$\dot{m}_{6'} = \dot{m}_7$	$h_{6'} = h_7$
ORCT	$\dot{m}_{10} = \dot{m}_{11}$	$\dot{m}_{10} h_{10} = \dot{m}_{11} h_{11} + \dot{W}_t$
ORCcon	$\dot{m}_{11} = \dot{m}_{12}$	$\dot{Q}_{ORC,con} = \dot{m}_{10}(h_{11} - h_{12})$
FPSC	$\dot{m}_1 = \dot{m}_{2'}$	$\dot{Q}_y = \dot{m}_{2'} c_p (T_{2'} - T_1)$

where $\dot{m}$ $[kg/s], X(\%), T[℃], h[kJ/kg], \dot{W}_p[kW], \dot{W}_t$ $[kW], c_p, \dot{Q}$ $[kW]$, and f are mass flow rate, LiBr concentration in solution, temperature, specific enthalpy for streams, pump and turbine power, specific heat of working fluid, heat transfer rate and circulation rate, respectively.

3.2.2. Advanced exergy analysis

Advanced exergy analysis was performed to determine how much the component in the system can be advanced maximally and to determine how the progress in one component affects the performance of other components. In advanced exergy analysis, the exergy destruction rates were divided into four separate portions: endogenous, exogenous, unavoidable, and avoidable. These portions were determined with the Eqs. (4–6) (Mosaffa and Farshi, 2020):

To determine the endogenous exergy destruction rate, the exergy destruction was calculated for the situation where the examined component is in real conditions and other component is in ideal conditions by providing the same exergy product rate for the entire system. The unavoidable exergy destruction rate was estimated according to the defined unavoidable conditions for each component. Table 6 shows the real, ideal, and unavoidable conditions for each component. Also, in this analysis, unavoidable and avoidable exergy destruction rates were divided into endogenous and exogeneous parts with Eqs. (7–10):

From a deeper perspective, it has been seen that the exogeneous exergy destruction of any component is the sum of mexogeneous and contributions of exogeneous exergy destruction originating from other components in the system. The mexogeneous exergy destruction is a measure of simultaneous interactions among the components. This relation was expressed in Eq. (11).

In addition to these, the total avoidable exergy destruction rates for each component were estimated to realize the significance of the component from the thermodynamic improvement point of view utilizing Eq. (12):

3.3. Annual simulation of the proposed system in TRNSYS

Because the energy and exergy analyses made in the previous sections are instant analyses, they are not sufficient to measure the performance of the proposed system. The annual analysis of the proposed system in this study was made by modelling it in the TRNSYS program for an illustrative example of the city of Izmir, Turkey. The collector model in the TRNSYS is readily available but the absorption heat transformer and ORC system do not exist as a direct component. That is why the relevant components are integrated into calls via EES.

3.4. Economic consideration and comparison of the proposed system

The proposed system including the integration of the FPS, ORC, and absorptional heat transformer systems to present a more economical way for electricity production from solar energy was evaluated with economic considerations. In this economic evaluation, many parameters, such as total investment cost, payback period, net present value, internal rate of return, and levelized cost of electricity generation, were examined. These investigated parameters were also compared with existing solar power plants of similar scale and it was shown that this proposed system could be a strong alternative.

3.5. Exergoeconomic analyses

With exergoeconomic analysis, the concepts of exergy and economy were combined through the thermoeconomic cost flow and auxiliary equations defined for each component. Thus, the terms of exergy fuel, product, and destruction cost rates were determined. This analysis was also examined in two parts, conventional and advanced, as in the exergy analysis.

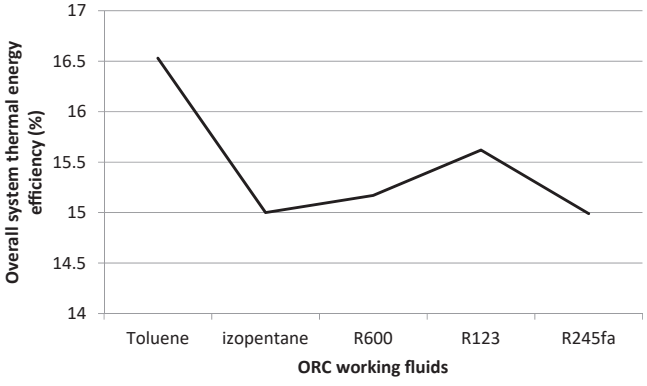

Fig. 2. Comparison results of thermal efficiency of overall proposed system for different selected ORC working fluids.

Table 4
Energy analysis results.

AHT cycle		ORC cycle		FPSC system	
Circulation ratio, f	19.15	Heat transfer rate in condenser, $\dot{Q}_{ORC,con}[kW]$	3582	Required heat transfer rate in collector, $\dot{Q}_y[kW]$	9930
Heat effect coefficient, $ITK[s/kJ]$	0.4614	Heat input rate in ORC cycle, $\dot{Q}_{in}[kW]$	4582	Required collector field area, $A[m^2]$	16027.142
Heat transfer rate in condenser, $\dot{Q}_{con}[kW]$	5348	Thermal efficiency of ORC system, η_{th}	0.2118		
Heat transfer rate in evaporator, $\dot{Q}_{ev}$ $[kW]$	4974				
Heat transfer rate in generator, $\dot{Q}_{gen}$ $[kW]$	4956				
Required pump powers, $\dot{W}_p$ $[kW]$	360.8				

Table 5
Exergy balance equations.

Equipment	Exergy balance equation
Gen	$\dot{E}x_{d,gen} = \dot{Q}_{gen}\left(1-\frac{T_0}{T_{gen}}\right) + \left[\dot{m}_7\dot{E}x_7 - \dot{m}_2\dot{E}x_2 - \dot{m}_8\dot{E}x_8\right]$
ABScon	$\dot{E}x_{d,con} = -\dot{Q}_{con}\left(1-\frac{T_0}{T_{con}}\right) + \left[\dot{m}_2\dot{E}x_2 - \dot{m}_3\dot{E}x_3\right]$
P1	$\dot{E}x_{d,P1} = \dot{W}_p + \left[\dot{m}_3\dot{E}x_3 - \dot{m}_4\dot{E}x_4\right]$
EV	$\dot{E}x_{d,ev} = \dot{Q}_{ev}\left(1-\frac{T_0}{T_{ev}}\right) + \left[\dot{m}_4\dot{E}x_4 - \dot{m}_5\dot{E}x_5\right]$
ABS	$\dot{E}x_{d,abs} = -\dot{Q}_{abs}\left(1-\frac{T_0}{T_{abs}}\right) + \left[\dot{m}_5\dot{E}x_5 + \dot{m}_9\dot{E}x_9 - \dot{m}_6\dot{E}x_6\right]$
SHX	$\dot{E}x_{d,SHX} = \left(\dot{m}_6\dot{E}x_6 - \dot{m}_9\dot{E}x_9\right)$
P2	$\dot{E}x_{d,P2} = \dot{W}_p + \left[\dot{m}_8\dot{E}x_8 - \dot{m}_9\dot{E}x_9\right]$
V	$\dot{E}x_{d,EV} = \left(\dot{m}_6\dot{E}x_6 - \dot{m}_7\dot{E}x_7\right)$
ORCT	$\dot{E}x_{d,T} = \left(\dot{m}_{11}\dot{E}x_{11} - \dot{m}_{10}\dot{E}x_{10}\right) - \dot{W}_t$
ORCcon	$\dot{E}x_{d,ORC,con} = -\dot{Q}_{ORC,con}\left(1-\frac{T_0}{T_{ORC,con}}\right) + \left[\dot{m}_{11}\dot{E}x_{11} - \dot{m}_{12}\dot{E}x_{12}\right]$
FPSC	$\dot{E}x_{d,FSC} = A_k I\left(1+\frac{1}{3}\left(\frac{T_0}{T_{solar}}\right)^4 - \frac{4}{3}\frac{T_0}{T_{solar}}\right) - \left[\dot{m}_{2'}c_p(T_{2'}-T_1) - T_0\ln\left(\frac{T_{2'}}{T_1}\right)\right]$

where $T_0[K]$, T_{solar} $[K]$, $A_k[m^2]$, $I[kW/m^2]$, $\dot{E}x$ $[kW]$, and $\dot{E}x_d$ $[kW]$ are dead-state and solar temperatures, cross-sectional area of solar collector, solar radiation density coming to the collector surface, exergy rate of streams and exergy destruction rates for equipment, respectively.

Table 6
Real, ideal, and unavoidable conditions for each component.

Component	Condition parameter	Real condition value	Ideal condition value	Unavoidable condition value
ABScon	Temperature difference, ΔT(°C)	55	0	20
P1	Isentropic efficiency, η_{P1}	0.918	1	0.95
EV	ΔT(°C)	0	0	0
ABS	ΔT(°C)	10	0	3
SHX	ΔT(°C)	0	0	0
P2	η_{P2}	1.202x10^{-9}	1	0.5
Gen	ΔT(°C)	4	0	2
ORCT	η_T	0.8	1	0.95
ORCcon	ΔT(°C)	0	0	0

3.5.1. Conventional exergoeconomic analysis

Table 7 indicates the defined thermoeconomic cost flow and auxiliary equations for each component. The investment cost rate term in this table was calculated with Eqs. (13–14) by implying the chemical component calculation method proposed by Smith (Smith, 2005):

Based on the fuel and product exergy (or exergetic fuel and product) rates for each component, the average costs per unit of product and fuel exergy, exergy destruction cost rate, and exergo-economic factor were computed with Eqs. (15–17).

3.5.2. Advanced exergoeconomic analysis

In advanced exergoeconomic analysis, exergy destruction and investment cost rates for each component were firstly divided into four parts: endogeneous, exogeneous, unavoidable, and avoidable, as in the advanced exergy analysis. The endogeneous cost rates originate from the components themselves. The exogeneous cost rates exist due to the impact of other components on special equipment. The unavoidable cost rates cannot be decreased due to technical limitations. However, the avoidable cost rates can be decreased with smarter equipment and/or structure optimization. These parts were calculated with Eqs. (18–33).

3.6. Environmental impact assessment

The environmental analysis was exerted on the proposed system for realizing the system whether is eco-friendly in terms of greenhouse gas emissions. In this evaluation, the total greenhouse gas emission quantity from the proposed system was obtained by summing direct and indirect emissions. To calculate the direct emissions, Eq. (34) (Hwang et al., 2015) was utilized:

To determine the indirect emission quantity, the components of energy consumption, equipment manufacturing, equipment recycling, and substance manufacturing emissions were added. Eqs. (35–39) were utilized for the estimation of total indirect equivalent CO_2 emission quantity.

3.7. Sustainability analysis

The sustainability indices, such as ecological effect, social-ecological

Table 7
Thermoeconomic cost flow and auxiliary equations.

Component	Thermo-economic cost equation	Auxiliary equation
ABScon	$c_2\dot{E}_2 + \dot{Z}_{ABScon} = c_3\dot{E}_3 + c_{\dot{Q}_{con}}\dot{E}_{\dot{Q}_{con}}$	$c_2 = c_3$
P1	$c_3\dot{E}_3 + c_{\dot{W}_{P1}}\dot{W}_{P1} + \dot{Z}_{P1} = c_4\dot{E}_4$	$c_{\dot{W}_{P1}} = c_{\dot{W}_{P2}} = c_T$
EV	$c_4\dot{E}_4 + \dot{Z}_{EV} + c_{\dot{Q}_{EV}}\dot{E}_{\dot{Q}_{EV}} = c_5\dot{E}_5$	$c_4 = c_5$
ABS	$c_5\dot{E}_5 + c_9\dot{E}_9 + \dot{Z}_{ABS} = c_6\dot{E}_6 + c_{\dot{Q}_{ABS}}\dot{E}_{\dot{Q}_{ABS}}$	$\frac{c_5\dot{E}_5 + c_9\dot{E}_9}{\dot{E}_5 + \dot{E}_9} = c_6$
SHX	$c_6\dot{E}_6 + \dot{Z}_{SHX} = c_9\dot{E}_9$	
P2	$c_8\dot{E}_8 + c_{\dot{W}_{P2}}\dot{W}_{P2} + \dot{Z}_{P2} = c_9\dot{E}_9$	$c_8 = c_9$
Gen	$c_7\dot{E}_7 + c_{\dot{Q}_{Gen}}\dot{E}_{\dot{Q}_{Gen}} + \dot{Z}_{Gen} = c_2\dot{E}_2 + c_8\dot{E}_8$	$\frac{c_2\dot{E}_2 + c_8\dot{E}_8}{\dot{E}_2 + \dot{E}_8} = c_7$
ORCT	$c_{10}\dot{E}_{10} + \dot{Z}_T = c_{11}\dot{E}_{11} + c_T\dot{W}_T$	$c_{10} = c_{11}$
ORCcon	$c_{11}\dot{E}_{11} + \dot{Z}_{ORCcon} = c_{12}\dot{E}_{12} + c_{\dot{Q}_{ORCcon}}\dot{E}_{\dot{Q}_{ORCcon}}$	$c_{11} = c_{12}$
FPSC	$c_0\dot{E}_0 + \dot{Z}_{FPSC} = c_1\dot{E}_1$	$c_0 = c_1$

where $c(\$/kWh)$, $\dot{E}$ (kW), and $\dot{Z}(\$/h)$ are cost rate associated with exergy streams, exergy rates for streams and heat and work interactions, and investment cost rate, respectively.

Table 8
Environmental and sustainability analysis results.

Component	*EcoEF*	*EEF*	*EXSI*	*SEF*
Gen	2.028	1.028	0.9726	1.972
ABScon	1.276	0.2991	3.343	4.63
P1	9.551	8.55	0.117	1.117
EV	1.088	0.0884	11.31	12.32
ABS	2.471	1.471	0.6798	1.68
SHX	1.056	0.05633	17.75	18.76
P2	3.774	2.774	0.3605	1.361
V	1.026	0.02642	37.85	38.91
ORCT	1.05	0.04971	20.12	21.1
ORCcon	1.309	0.3086	3.241	4.241
FPSC	78.8	77.83	0.01285	1.013
Overall system	1.05	0.1022	9.787	21.05

factors, and exergetic sustainability index (Balli and Caliskan, 2021), were estimated for the proposed system with Eqs. (40–42). The environmental and sustainability analysis results are shown in Table 8.

3.8. Novel indices developed based on the advanced exergy analysis

In the previous sections, it was stated that the energy, advanced exergy, and advanced exergoeconomic analyses available in the literature were carried out for the proposed system in this study. However, with advanced exergy analysis, it is a fact that more detailed information was obtained for the development potential both for the system and all components separately. For this reason, the novel indices developed based on the advanced exergy analysis by considering the parameters and assumptions of this analysis in a more detailed manner are shown in Table 9. This table includes the name, representation, and purpose of the utilization of developed novel indices. The relationships between the developed novel indices were expressed with Eqs. (43–61). The mathematical basis of the relations between the novel indices was established with Eqs. (62–65).

3.9. Novel prioritization method developed for the improvement potential of the proposed system

Table 10 illustrates the general methodology of the developed novel prioritization method based on the novel indices for estimation and implementation of the improvement potential of the system.

3.10. Validation of novel prioritization method and performance metrics

To prove the accuracy of the developed novel prioritization method and performance metrics, first of all, a previously published study on energy systems was selected from the literature (Zhou et al., 2021), and then the novel methodology was applied to this study while the results were compared. The required data for implementation of the novel methodology on the reference study was obtained by forming the thermodynamic model of the pertained study from the design parameters, and applying energy and advanced exergoeconomic analyses on this system. In Table 11, the performance assessment conclusions with novel indices are presented for reference study. By evaluating the *UPI* value in Table 11 and advanced exergoeconomic results, the novel prioritization methods was implemented on this study. The conclusions of the novel prioritization method indicate that the greatest irreversibility occurs in the evaporator due to thermal reactions in the reference system which consists of ORC and absorption refrigeration system components although the improvement potential of this component is quite low. However, the turbine and absorber have high improvement potential in the overall thermodynamic betterment of the system, and these components should be prioritized by the implementation of relevant equipment condition optimization. These findings are fully consistent with the results of the reference study.

4. Results and discussion

4.1. Exergy analysis results

4.1.1. Conventional exergy analysis results

In Fig. 3, the overall exergetic efficiency values for the five different ORC working fluids were compared to estimate the best working fluid from the exergetic point of view. The conventional exergy analysis results for the proposed system for the best working fluid of R123 are shown in Table 12 and Fig. 4. It is clear from the results in the table that the entire exergy destruction rate for the proposed system is 5853.89 kW. Fig. 4 presents the distribution of exergy destruction of the entire system based on each component percentile. According to the figure, SHX and FPSC were the components that contributed the highest to the exergy destruction with 23.711% and 21.849%, respectively. On the other hand, ORCcon and ORCT had the lowest exergy destruction rate with 0.242% and 0.849%, respectively. Based on these observations, the component improvement priority chart is introduced in Table 13.

4.1.2. Advanced exergy analysis results

The advanced exergy analysis results of the proposed system are indicated in Tables 13–15 and Figs. 3–4. The endogenous, exogeneous, unavoidable, and avoidable exergy destruction rates of the components

Table 9
Descriptive list of the developed novel indices.

Name	Representation	Purpose of utilization
Specific internal irreversibility generation index	*SIIG*	To express that how much internal irreversibility constitutes in the overall system per unit total exergy product rate
Specific external irreversibility generation index	*SEIG*	To state that how much external irreversibility constitutes in the overall system per unit total exergy product rate
Equipmentwise endogeneous exergetic efficiency	$\eta_{ex,EN}$	To estimate the exergetic efficiency of equipment for endogeneous conditions
Equipmentwise exogeneous exergetic efficiency	$\eta_{ex,EX}$	To account the exergetic efficiency of equipment for exogeneous conditions
Internal exergy fuel ratio	*IExFR*	To evaluate the impact of internal irreversibilities on the fuel exergy rate
Internal mass flow ratio	*IMFR*	To examine the impact of internal irreversibilities on the mass flowrate
External to internal exergy product ratio	*ETIExPR*	To assess the significance degree of external and internal irreversibilities comparatively
Unavoidable exergetic efficiency	$\eta_{ex,UN}$	To determine the exergetic efficiency of equipment for unavoidable conditions
Avoidable exergetic efficiency	$\eta_{ex,AV}$	To calculate the exergetic efficiency of equipment for avoidable conditions
Unavoidable exergy fuel ratio	*UNExFR*	To investigate the impact of unavoidable irreversibilities on the fuel exergy rate
Unavoidable exergy product ratio	*UNExPR*	To mean the impact of unavoidable irreversibilities on the product exergy rate
Avoidable exergy fuel ratio	*AVExFR*	To determine the impact of avoidable irreversibilities on the fuel exergy rate
Avoidable exergy product ratio	*AVExPR*	To estimate the impact of avoidable irreversibilities on the product exergy rate
Upgrade potential index	*UPI*	To state the ratio of feasible recoverable to the unrecoverable exergy destruction rates due to the technological and economical limitations

Table 10
General methodology of the developed novel prioritization method.

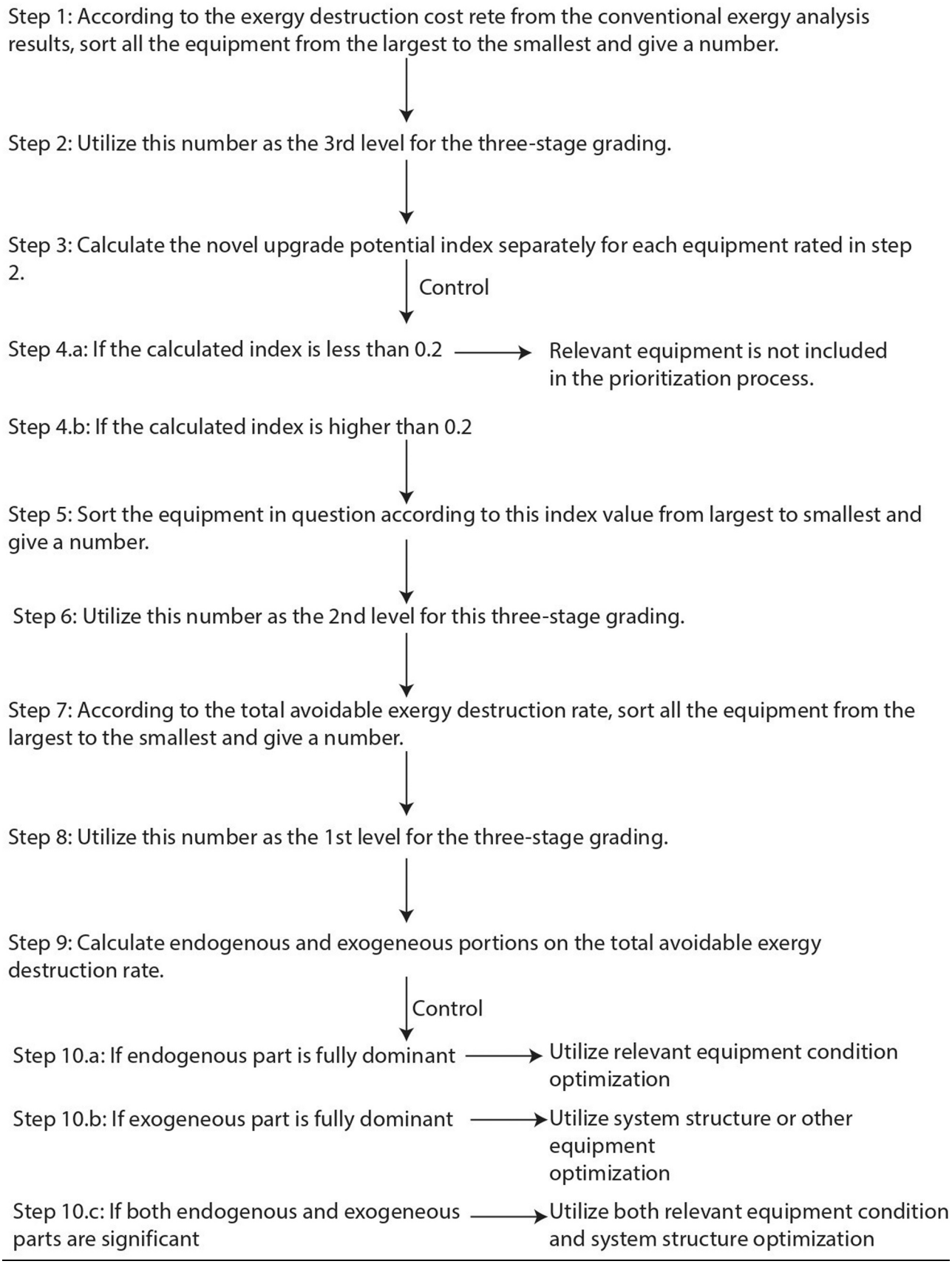

Table 11
Performance evaluation results based on the developed novel indices for reference study of (Zhou et al., 2021).

Component, k	$\eta_{ex,EN,k}$	$\eta_{ex,EX,k}$	$\eta_{ex,UN,k}$	$\eta_{ex,AV,k}$	$ETIExPR,k$	$UNExFR,k$	$AVExFR,k$	$UNExPR,k$	$AVExPR$	UPI
Evaporator 1	0.613	0.387	0.429	0.571	0.173	0.864	0.031	0.864	0.136	0.255
Turbine	0.466	0.534	0.326	0.674	0.237	0.468	0.036	0.468	0.532	0.646
Condenser 1	0.760	0.240	0.532	0.468	0.302	0.316	0.356	0.316	0.684	0.549
Pump 1	0.927	0.073	0.649	0.351	0.267	0.136	0.738	0.136	0.864	0.516
Generator	0.835	0.165	0.584	0.416	0.213	0.877	0.082	0.877	0.123	0.396
Condenser 2	0.596	0.404	0.417	0.583	0.293	0.182	0.149	0.182	0.818	0.615
Absorber	0.262	0.738	0.183	0.817	0.093	0.673	0.156	0.673	0.327	0.763
Pump 2	0.851	0.149	0.595	0.405	0.105	0.298	0.492	0.298	0.702	0.527
Heat exchanger	0.729	0.271	0.510	0.490	0.846	0.662	0.155	0.662	0.338	0.506

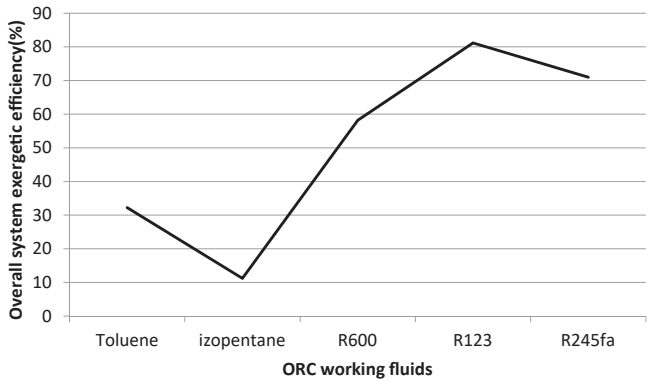

Fig. 3. Comparison results of exergy efficiency of overall proposed system for different selected ORC working fluids.

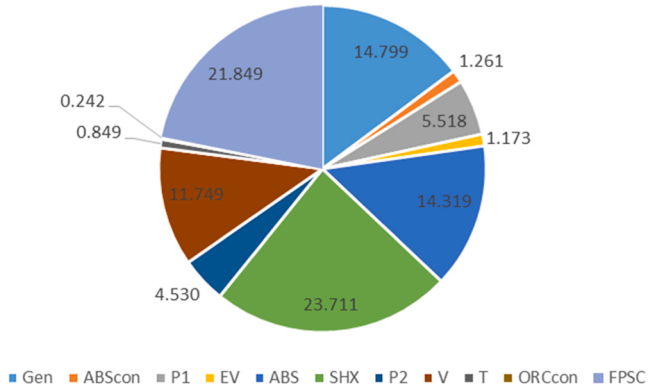

Fig. 4. Distribution of exergy destruction rates of entire system based on each component percentile.

are summarized in Table 14 while Table 15 shows the unavoidable and avoidable components of endogenous and exogeneous exergy destruction rates of the components. Table 16 illustrates the contributions of other system components to exogeneous exergy destruction rates of each component. The unavoidable and avoidable exergy destruction share of each component over entire exergy destructions is also shown in Fig. 5. According to Fig. 5, only for P1 and FPSC, the avoidable exergy destruction was become higher than the unavoidable one. For all other components, the unavoidable part dominated, particularly for the evaporator (EV), SHX, P2, and ORC turbine (ORCT), where the unavoidable part of the exergy destruction is over 95% of total exergy destruction within these components. Also, FPSC and P1 constituted the highest and middest avoidable exergy destruction values within the overall components. The endogenous and exogeneous exergy destruction shares of each component are presented in Fig. 6 where the exogeneous exergy destruction component is dominated by the endogenous one for only SHX and P2. This situation explained that these components are stronger. For all other components, the endogenous part dominated, particularly for the ABS where the endogenous part of exergy destruction is over 85% of the entire exergy destruction within this component.

Table 13
Component improvement priority chart according to the conventional exergy analysis results.

		Degree
First priority	SHX	1
	FPSC	2
	Gen	3
	ABS	4
	V	5
Second priority	P1	1
	P2	2

Also, in P1, EV, ABScon, and generator (Gen), endogenous and exogeneous parts were quite closer. From the results in Table 16, it is obvious that Gen, V, and ORCcon were the biggest contributors to exogenous exergy destruction of almost all components. Also, mexogeneous components had quite an important share for ABScon, P1, and EV. This expressed that the simultaneous interactions among these components were stronger. In these components, commonly simultaneous

Table 12
Conventional exergy analysis results.

Component	Product exergy rate, $\dot{E}x_P$ $[kW]$	Fuel exergy rate, $\dot{E}x_F$ $[kW]$	Exergy destruction rate, $\dot{E}x_D$ $[kW]$	Exergetic efficiency, η_{ex}	Overall system exergetic efficiency, $\eta_{ex.OAS}$
Gen	842.3	1709	866.3	0.493	
ABScon	267.9	314.8	73.83	0.784	
P1	37.77	360.8	323	0.1047	
EV	776.8	845.5	68.67	0.9188	
ABS	569.8	1408	838.2	0.4047	
SHX	24642	26030	1388	0.9467	
P2	95.61	360.8	265.2	0.265	
V	26030	26718	687.8	0.9743	
ORCT	1000	1050	49.72	0.9526	
ORCcon	45.92	60.09	14.17	0.7642	
FPSC	16.43	1295	1279	0.01269	0.9525

Table 14
Endogenous, exogeneous, unavoidable, and avoidable exergy destruction rates of each component.

Equipment	$\dot{E}_{D,k}^{EN}[kW]$	$\dot{E}_{D,k}^{EX}[kW]$	$\dot{E}_{D,k}^{UN}[kW]$	$\dot{E}_{D,k}^{AV}[kW]$
Gen	560.5	305.8	497.9	368.4
ABScon	53.43	20.4	387.1	-313.3
P1	230.3	92.71	104.4	218.6
EV	48.96	19.71	68.67243	-0.00243
ABS	734.6	103.6	1933	-1095
SHX	269.8	1118	1384	3.663
P2	2.985	262.2	239.3	25.9
V	817.9	-130.1	679.3	8.493
ORCT	187.6	-137.9	49.72	0.00195
ORCcon	98.94	-84.77	184.2	-170
FPSC	1372	-92.66	45.15	1234

Table 15
Unavoidable and avoidable components of endogenous and exogeneous exergy destruction rates of each component.

Component	$\dot{E}_{D,k}^{UN,EN}[kW]$	$\dot{E}_{D,k}^{UN,EX}[kW]$	$\dot{E}_{D,k}^{AV,EN}[kW]$	$\dot{E}_{D,k}^{AV,EX}[kW]$
Gen	412.6	85.32	147.9	220.5
ABScon	280.1	107	-226.6	-86.68
P1	74.44	29.96	155.9	62.74
EV	48.96	19.71	0.003453	-0.005883
ABS	1173	760	-438.4	-656.6
SHX	4.422	1380	265.4	-261.7
P2	2.243	197.1	0.742	65.15
V	650.6	28.66	167.3	-158.8
ORCT	4.973	44.75	182.6	182.59805
ORCcon	-96.17	280.4	195.1	-365.1
FPSC	57.46	-12.31	1315	-80.54

interaction of ABS, P2, V, FPSC, and ORCcon existed. Hence, this situation was consistent. In this table, the negative value terms indicated the situation of enhancing exergy destruction of the *kth* component with decreasing the exergy destruction of the *rth* component. This situation occurred for P1 on ABSCon, EV on ABScon and ABS, ABS on ABScon, V on ABScon, ORCcon on ABScon, P1, EV, ABS and Gen, Gen on P1, EV, ABS and SHX, SHX on ABS, P2 and Gen, P2 on ABS, SHX, and Gen, ORCT on P2, FPSC on P2, and ABScon on P2. The strongest and weakest impacts of irreversibilities were due to Gen on SHX and ABScon on P2, respectively. From this observation, we concluded that due to the existence of chemical and thermal reactions, Gen and ORCcon had the most influential irreversibilities, which also triggered the exogeneous exergy destruction of other components strongly. Hence, the Gen and ORCcon temperatures should be optimized primarily.

4.2. Annual simulation results in TRNSYS

The annual electricity production simulation results from TRNSYS are shown in Fig. 7. According to the simulation in TRNSYS, the total annual electricity generation is calculated as 2601 MWh.

4.3. Economic consideration results and comparison of the proposed system with existing small-medium scaled solar power plants

The economic evaluation results of the proposed system are shown in Table 17. To compare the proposed system in terms of generated electricity output and economic variables with similar scaled existing solar power plants, Saguaro, Rende, Iresen, and Ougadougou ORC solar power plants (Permana et al., 2022) for 1000 kW of net turbine power are considered. When the compared solar power plants are modeled with TRNSYS, it is determined that the annual electricity generation is between 2000 and 2200 MWh. However, with the proposed system, it has been shown that 2601 MWh of electricity can be produced annually for the example of Izmir city in Turkey. This is due to both the difference in the normal solar radiation level in the location where the simulation is performed and the process of raising the temperature of the heat source due to the FPS and ORC integration in our proposed system. On the other hand, it has been determined that the total initial investment costs of the compared solar power plants are in the range of approximately US$6–10 million, and the payback periods vary between 10 and 15 years. For the proposed system, these values were determined as US$3.924 million and 4.531 years, respectively. These values have proven that the cost burden of solar collectors in the entire system can be alleviated in the production of electricity with solar energy with the proposed system. Therefore, we think that the proposed system is a powerful alternative for generating electricity from solar energy more economically.

4.4. Exergoeconomic analysis results

4.4.1. Conventional exergoeconomic analysis

The conventional exergoeconomic results of the proposed system are shown in Table 18 and Fig. 8. According to these, the total investment and exergy destruction cost rates were 250.526 US$/h and 231.229 US $/h, respectively. Investment cost rates were evenly distributed among almost all the components due to the provision of needed heat for the generator and evaporator via low-grade solar energy. However, exergy destruction cost rates were concentrated in Gen, FPSC, and SHX with percentages of 67.59, 59.09, and 47.98, respectively. This is because strong thermal and/or chemical processes take place in these components.

4.4.2. Advanced exergoeconomic analysis

The advanced exergoeconomic results of the proposed system are illustrated in Tables 19 and 20 and Figs. 9–11. The advanced components of investment and exergy destruction cost rates are presented in these two tables, respectively. The distribution of overall exergy destruction cost rate components (UNEN, UNEX, AVEN, AVEX) based on each component in Fig. 9 supported the results of advanced exergy analysis. Fig. 10 summarizes the percent of investment cost rate components to the overall system for each component. The distribution of investment cost rate components over the considered component is shown in Fig. 11 where on average 67.504% of the investment cost rate for all components except P1 and SHX are due to the unavoidable endogenous component. In P1, avoidable endogenous investment cost rate was 54.701% of the overall cost rate. This meant that component could achieve high improvement potential by optimizing conditions. This was also valid for SHX, EV, ABS, Gen, ORCT, and ORCcon. However, in P2, and FPSC, the avoidable exogeneous rate was substantial. This situation involves system structure or other component optimization for achieving higher improvement potential in that component.

4.5. Environmental impact and sustainability analysis results

The environmental impact and sustainability analysis results of the proposed system are shown in Tables 21 and 22. According to the results levelized power output capacity equivalent CO_2 emission is 0.1022 t/MWh. This value is in the range of 0.4 and 0.6 in the previous literature studies for similar scale solar power plants (Bet Sarkis and Zare, 2018; Jie Ling et al., 2022). This situation comes from the utilization of clean energy technologies with higher exergetic efficiency and lower economic costs. Hence, the proposed system forms a good alternative to classic solar power plants in terms of exergo-environmental aspect.

4.6. Performance evaluation and improvement potential results

The proposed system was evaluated with the defined conventional and novel performance parameters completely developed by the authors. For conventional performance parameters, the results are shown in Table 23. However, Table 24 presents the performance evaluation results based on the novel indices. In addition, the novel prioritization method proposed in section 2.9 was also applied to this system. As a

Table 16
Contribution of other system components to exogeneous exergy destruction rates of each component.

Component,k	$\dot{E}_{D,k}^{EX}$[kW]	Component, r	$\dot{E}_{D,k}^{EX,r}$[kW]	Component, k	$\dot{E}_{D,k}^{EX}$[kW]	Component, r	$\dot{E}_{D,k}^{EX,r}$[kW]
ABScon	20.4	P1	-0.79	G	305.8	ABScon	225.4
		EV	-0.79			P1	87.1
		ABS	-0.79			EV	166.6
		SHX	7.38			ABS	86.9
		P2	0.07			SHX	-87
		V	-0.35			P2	-180.1
		G	32.33			V	-86.9
		T	0.06			T	44.3
		ORCcon	-20.71			ORCcon	-190.3
		FPSC	-0.79			FPSC	225.4
P1	92.71	ABScon	35.7				
		EV	35.7				
		ABS	35.7				
		SHX	35.7				
		P2	35.4				
		V	21.9				
		G	-78.8				
		T	18.2				
		ORCcon	-93.4				
		FPSC	35.7				
EV	19.71	ABScon	7.59				
		P1	7.59				
		ABS	7.59				
		SHX	7.59				
		P2	7.53				
		V	16.71				
		G	-16.75				
		T	3.83				
		ORCcon	-19.85				
		FPSC	-7.59				
ABS	103.6	ABScon	113.9				
		P1	113.9				
		EV	-113.9				
		SHX	-113.9				
		P2	-122.1				
		V	604.9				
		G	-37				
		T	60				
		ORCcon	-297.4				
		FPSC	-113.9				
SHX	1118	ABScon	803.2				
		P1	803.2				
		EV	803.2				
		ABS	-803.2				
		P2	-1000				
		V	1630.2				
		G	-1634.2				
		T	732.2				
		ORCcon	-1035.2				
		FPSC	803.2				
P2	262.2	ABScon	-0.022				
		P1	0				
		EV	0				
		ABS	2.1178				
		SHX	-0.022				
		V	126.815				
		G	126.815				
		T	-0.004				
		ORCcon	0.762				
		FPSC	-0.022				

result of combining the performance evaluations with the novel prioritization methodology, it was seen that ABScon, P1, P2, ABS, Gen, and ORCcon component were of high development priority to improve the development potential of the whole system. Here, the components in question not only had a high exergy destruction rate in themselves due to the presence of strong thermal and/or chemical reactions, but also caused significant irreversibility for another component. Hence, to improve this proposed system from the thermodynamic point of view, both relevant component conditions and system structure optimization should be applied. Another point to be considered here is that ABS and Gen components exhibited opposite behavior in terms of exergy destruction activities.

5. Conclusions

In this present study, a novel ORC system assisted with low-grade solar energy, FPS, and AHT systems was proposed to provide electricity generation. With this novel process design, it was aimed at achieving a potent production output more economically by combining two robust system technologies, such as ORC and AHT, with a renewable energy source, unlike existing small-medium-sized solar power plants. To compare the techno-economic data of the proposed system with other

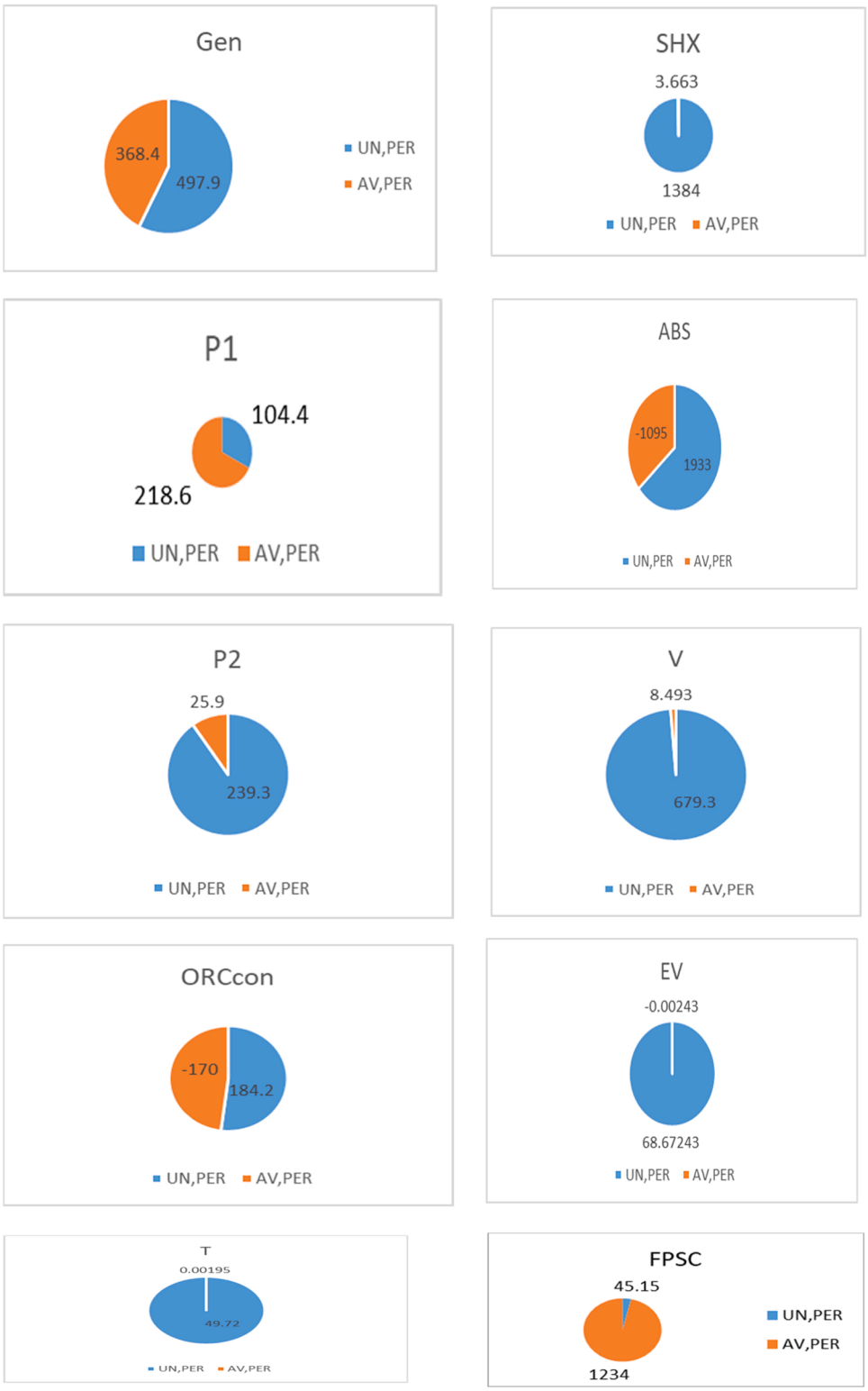

Fig. 5. Unavoidable and avoidable exergy destruction percentages of each component over entire exergy destruction.

solar power plants of similar capacities in the world, the proposed system was modeled in EES and TRNSYS for an illustrative example of the city of Izmir, Turkey. According to the results of this comparison, it has been estimated that the proposed system for 1000 kW turbine power draws attention with its lower investment cost and payback period compared to its counterparts in the world. Hence, the proposed system forms a stronger alternative for electricity production from solar energy in a more economical way. The conventional and advanced exergy, exergoeconomic, environmental impact, and sustainability analyses were implemented on this proposed system to bring to light the hints for improvement of this system from the thermodynamic point of view. This proposed system was examined by the defined conventional and novel performance parameters completely developed by the authors. These novel performance indices were derived based on the advanced exergy

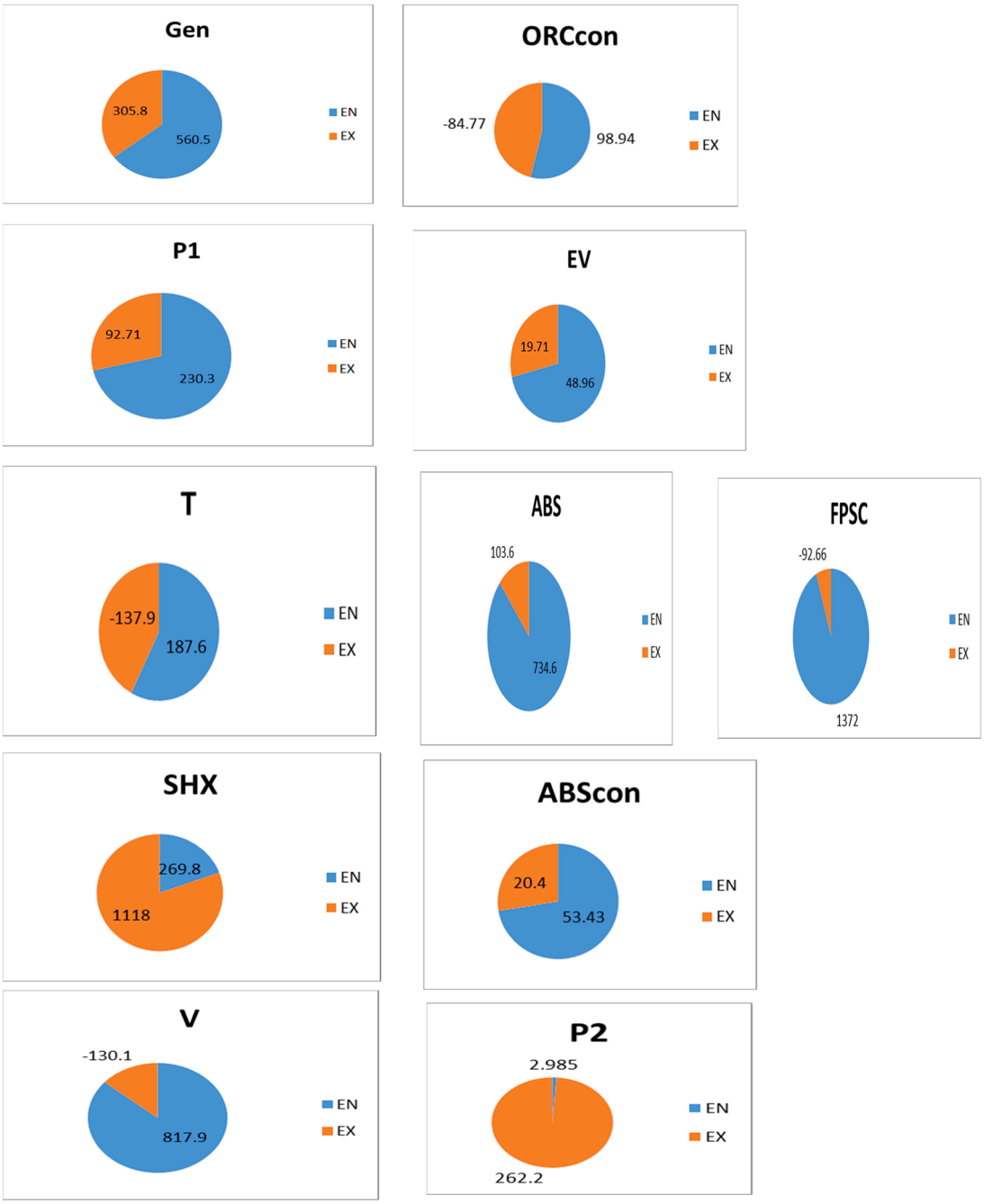

Fig. 6. Endogenous and exogeneous exergy destruction percentages of each component over entire exergy destruction.

analysis to reveal the feasible improvement potential of both any component and the entire system from a deeper perspective. Unlike the performance indices available in the literature, it has been suggested which equipment should be prioritized in improving the overall performance of the system with these indices, together with a numerical value. Based on these novel indices, the novel prioritization method with a three-stage rating system was presented step by step to assess and imply the improvement potential of the system. With this novel method, not only the improvement potentials of the equipment were graded, but also what kind of improvement model should be used for each of them was also specified. The key conclusions of the study may be listed as follows:

a) Conventional exergy analysis results showed that the total exergy destruction rate was 5853.89 kW. The highest exergy destruction rates were contributed by SHX (23.711%) and FPSC (21.849%), while ORCcon and ORCT had the lowest rates with 0.242% and 0.849% respectively.
b) Advanced exergy analysis highlighted the potential for improvement in FPSC and P1 due to dominant avoidable exergy destruction rates. SHX and P2 exhibited stronger irreversibilities with exogeneous parts dominating at 80.562% and 98.874% respectively. Gen, V, and ORCcon were major contributors to exogenous exergy destruction but showed adverse aspects. Hence, the temperatures of Gen and ORCcon should be optimized quite carefully.
c) Conventional exergoeconomic analysis indicated total investment and exergy destruction cost rates are 250.526 US$/h and 231.229 US $/h respectively. Gen, FPSC, and SHX had higher exergy destruction cost rates due to stronger thermal and/or chemical processes.

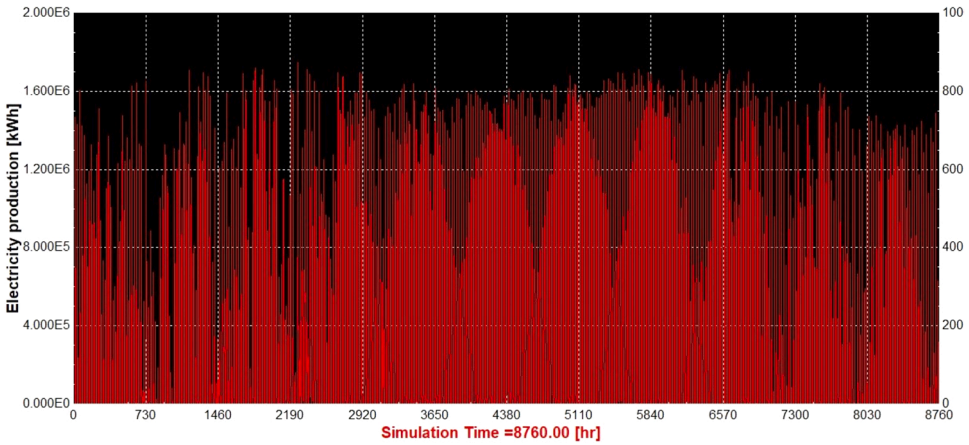

Fig. 7. Annual electricity production simulation of the proposed system in TRNSYS for an illustrative example of Izmir, Turkey.

Table 17
Economic evaluation results of the proposed plant.

Installed cost of FPSC	96 US$/m^2
ORC power plant cost	US$503241.827
AHT cycle cost	US$187488.779
Total direct cost	US$3678751.938
Total indirect cost	US$245250.1292
Total cost	US$3924002.067
Fixed O&M cost by capacity	9 US$/kWh
Variable O&M cost by generation	0.343 US$/MWh
Revenue for electricity selling	876000 US$/year
Operating expenses	9892.143 US$/year
Annual net cash flow	866107.857 US$/year
Payback period	4.531 years
Net present value	US$4878251.845 (for 20 years of useful lifetime)
Levelized cost of electricity generation	0.342 US$/kWh
Internal rate of return	13.38%

Table 18
Conventional exergoeconomic analysis results.

Component	c_f (US$/GJ)	c_p (US$/GJ)	$\dot{C}_d$ (US$/h)	f_k
ABScon	11.72	13.53	3.116	0.307
P1	14.13	13.53	16.43	0.551
EV	1.184	13.53	0.2926	0.992
ABS	1.774	13.53	5.353	0.776
SHX	13.53	13.53	67.59	0.499
P2	19.1	13.53	18.24	0.525
Gen	15.38	13.53	47.98	0.196
ORCT	43.03	52.95	7.702	0.784
ORCcon	106.5	43.03	5.435	0.847
FPSC	2.44	186.5	59.09	0.626

However, the investment cost rates were distributed smoothly due to the renewable energy integration.

d) Advanced exergoeconomic analysis supported the above results, revealing that the unavoidable endogenous part for investment cost rate had an average share of 67.504% in most components. Some components like ABS, Gen, ORCT, P1, and SHX had different dominance patterns, requiring system structure optimization.

e) The proposed system forms a good alternative to classic solar power plants in terms of exergo-environmental aspect

f) With the implementation of a novel prioritization method on this proposed system, it was realized that P1, P2, ABScon, ABS, Gen, and ORCcon had high development priorities to improve overall the system. However, within these components, Gen and ORCcon had a high priority degree for the overall system.

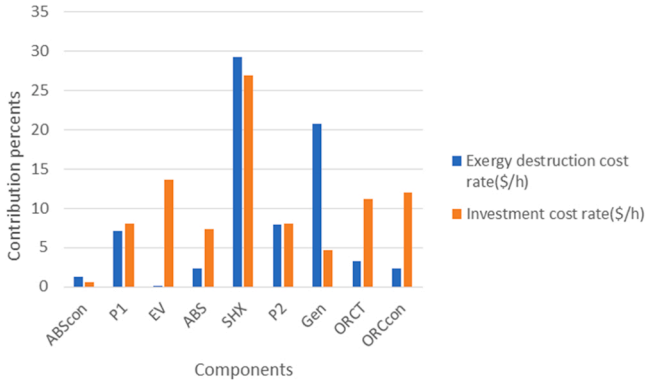

Fig. 8. Investment and exergy destruction cost rate distribution based on each component percentile from conventional exergoeconomic analysis results.

As a result of this study, it has been determined that the proposed system for 1000 kW turbine power draws attention with its lower investment cost and payback period compared to its counterparts in the world.

Formulae

$$\dot{E}^{Ph} = \dot{m}[(h_i - h_0) - T_0(s_i - s_0)] \quad (1)$$

$$\dot{E}^{Ch} = \sum z_i b_i \quad (2)$$

$$\dot{E} = \dot{E}^{Ph} + \dot{E}^{Ch} \quad (3)$$

$$\dot{E}_{D,k} = \dot{E}_{D,k}^{EN} + \dot{E}_{D,k}^{EX} \quad (4)$$

$$\dot{E}_{D,k} = \dot{E}_{D,k}^{UN} + \dot{E}_{D,k}^{AV} \quad (5)$$

$$\dot{E}_{D,k}^{UN} = \dot{E}_{P,k}^{real}\left(\frac{\dot{E}_{D,k}}{\dot{E}_{P,k}}\right)^{UN} \quad (6)$$

$$\dot{E}_{D,k}^{UN,EN} = \dot{E}_{P,k}^{EN}\left(\frac{\dot{E}_{D,k}}{\dot{E}_{P,k}}\right)^{UN} \quad (7)$$

$$\dot{E}_{D,k}^{UN,EX} = \dot{E}_{D,k}^{UN} - \dot{E}_{D,k}^{UN,EN} \quad (8)$$

$$\dot{E}_{D,k}^{AV,EN} = \dot{E}_{D,k}^{EN} - \dot{E}_{D,k}^{UN,EN} \quad (9)$$

$$\dot{E}_{D,k}^{AV,EX} = \dot{E}_{D,k}^{AV} - \dot{E}_{D,k}^{AV,EN} \quad (10)$$

Table 19
Advanced components of investment cost rates for each component.

Component	$\dot{Z}$ (US$/h)	$\dot{Z}^{EN}$ (US$/h)	$\dot{Z}^{EX}$ (US$/h)	$\dot{Z}^{UN}$ (US$/h)	$\dot{Z}^{AV}$ (US$/h)	$\dot{Z}^{UN,EN}$ (US$/h)	$\dot{Z}^{UN,EX}$ (US$/h)	$\dot{Z}^{AV,EN}$ (US$/h)	$\dot{Z}^{AV,EX}$ (US$/h)
ABScon	1.379	0.9985	0.3802	1.374	0.00444	1.049	0.325	-0.051	0.0552
P1	20.192	11.55	8.638	9.085	11.11	0.507	8.578	11.043	0.06
EV	34.220	29.53	4.692	34.22	-0.002	24.4	9.82	5.13	-5.128
ABS	18.583	9.943	8.64	7.036	11.55	7.258	-0.222	2.685	8.862
SHX	67.391	20.8	46.59	65.79	1.605	0.2101	65.580	20.590	-18.990
P2	20.192	26.79	-6.599	21.66	-1.47	52.57	-30.91	-25.78	24.311
Gen	11.676	7.704	3.971	8.2	3.476	5.967	2.233	1.737	1.738
ORCT	27.950	17.78	10.17	4.014	23.94	4.014	0	13.766	10.17
ORCcon	30.163	28.39	1.778	30.13	0.031	27.34	2.79	1.05	-1.012
FPSC	18.780	13.39	5.393	10.23	8.546	13.02	-2.79	0.37	8.183

Table 20
Advanced components of exergy destruction cost rates for each component.

Component	$\dot{C}_d$ (US$/h)	$\dot{C}_d^{EN}$ (US$/h)	$\dot{C}_d^{EX}$ (US$/h)	$\dot{C}_d^{UN}$ (US$/h)	$\dot{C}_d^{AV}$ (US$/h)	$\dot{C}_d^{UN,EN}$ (US$/h)	$\dot{C}_d^{UN,EX}$ (US$/h)	$\dot{C}_d^{AV,EN}$ (US$/h)	$\dot{C}_d^{AV,EX}$ (US$/h)
ABScon	3.116	2.255	0.8611	16.34	-13.22	11.82	4.516	-9.565	-3.659
P1	16.43	10.34	4.716	5.311	11.12	3.787	1.524	7.93	3.191
EV	0.2926	0.2086	0.08399	0.2926	-0.00001	0.2086	0.08399	0.00001471	-0.00002
ABS	5.353	4.691	0.6616	12.34	-6.993	7.491	4.854	-2.8	-4.193
SHX	67.59	13.14	54.44	67.4	0.1784	0.2153	67.2	12.92	-12.74
P2	18.24	0.2053	18.03	16.46	1.781	0.1543	13.56	0.0510	4.481
Gen	47.98	31.04	16.94	27.58	20.4	22.85	4.725	8.191	12.21
ORCT	7.702	29.06	-21.36	7.702	0.0003	0.7704	6.933	28.29	28.29
ORCcon	5.435	37.95	-32.51	70.65	-65.21	-36.89	107.6	74.83	-140
FPSC	11.23	12.05	-0.8138	0.3966	10.84	0.5047	-0.1081	0.1155	-0.707

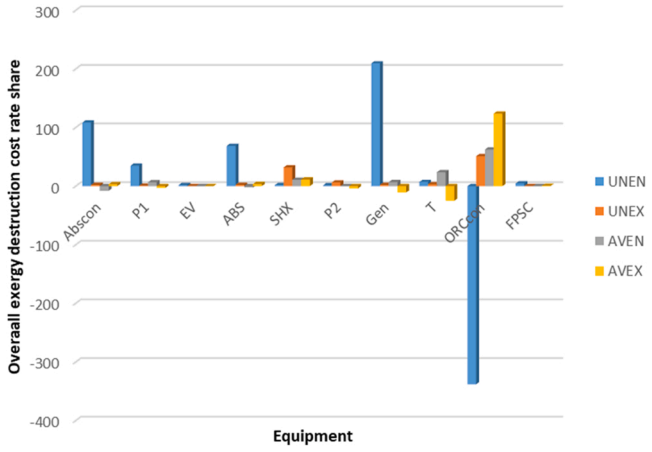

Fig. 9. Distribution of overall exergy destruction cost rate components (UNEN, UNEX,AVEN,AVEX) based on each component.

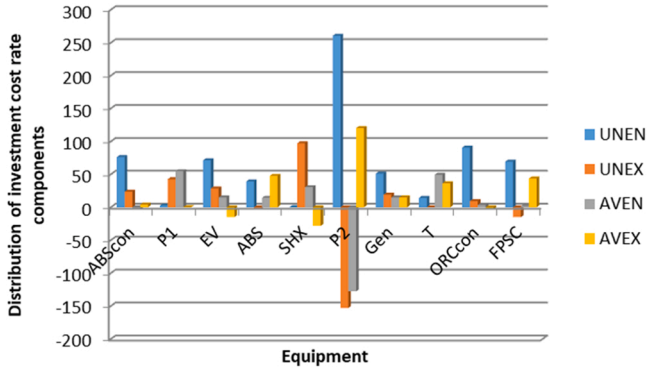

Fig. 10. For each component the percent of advanced investment cost rate components to overall system.

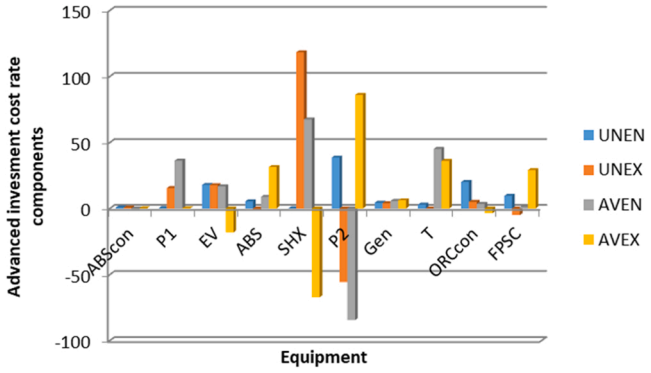

Fig. 11. Distribution of investment cost rate components over the considered component.

Table 21
Environmental impact analysis results.

Total CO_2 emission from the proposed plant (kg)	265.748
Levelized power output capacity equivalent CO_2 emission (t/MWh)	0.102

$$\dot{E}_{D,k}^{mexo} = \dot{E}_{D,k}^{EX} - \sum_{\substack{r=1 \\ r\neq k}}^{n-1} \dot{E}_{D,k}^{EX,r} \tag{11}$$

$$\dot{E}_{D,k}^{AV,T} = \dot{E}_{D,k}^{AV,EN} + \sum_{\substack{r=1 \\ r\neq k}}^{n} \dot{E}_{D,r}^{AV,EX,k} \tag{12}$$

$$\dot{Z} = \frac{\phi_k (CRF)\left(\frac{S_c}{S_b}\right)^M}{t} \frac{CEPCI_{2020}}{CEPCI_{2000}} r_m r_p r_t \tag{13}$$

Table 22
Sustainability analysis results.

Component	Ecological effect factor, *EcoEF*	Exergetic sustainability index, *EXSI*	Social ecological factor, *SEF*
Generator	2.028	0.9726	1.972
Absorptional heat transformer condenser	1.276	3.343	4.63
Pump 1	9.551	0.117	1.117
Evaporator	1.088	11.31	12.32
Absorber	2.471	0.6798	1.68
Solution heat exchanger	1.056	17.75	18.76
Pump2	3.774	0.3605	1.361
Expansion valve	1.026	37.85	38.91
Turbine	1.05	20.12	21.1
ORC condenser	1.309	3.241	4.241
Flat plate solar collector	78.8	0.01285	1.013
Overall system	1.05	9.787	21.05

$$CRF = \frac{i(1+i)^N}{(1+i)^N - 1} \tag{14}$$

$$c_p \dot{E}_p = c_f \dot{E}_f + \dot{Z} \tag{15}$$

$$\dot{C}_d = c_f \dot{E}_d \tag{16}$$

$$f = \frac{\dot{Z}}{\dot{Z} + \dot{C}_d} \tag{17}$$

$$\dot{C}_{d,k}{}^{EN} = c_{f,k} \dot{E}_{d,k}{}^{EN} \tag{18}$$

$$\dot{C}_{d,k}{}^{EX} = c_{f,k} \dot{E}_{d,k}{}^{EX} \tag{19}$$

$$\dot{C}_{d,k}{}^{UN} = c_{f,k} \dot{E}_{d,k}{}^{UN} \tag{20}$$

$$\dot{C}_{d,k}{}^{AV} = c_{f,k} \dot{E}_{d,k}{}^{AV} \tag{21}$$

$$\dot{C}_{d,k} = \dot{C}_{d,k}{}^{EN} + \dot{C}_{d,k}{}^{EX} \tag{22}$$

$$\dot{C}_{d,k} = \dot{C}_{d,k}{}^{UN} + \dot{C}_{d,k}{}^{AV} \tag{23}$$

$$\dot{C}_{d,k}{}^{UN,EN} = c_{f,k} \dot{E}_{d,k}{}^{UN,EN} \tag{24}$$

$$\dot{C}_{d,k}{}^{UN,EX} = c_{f,k} \dot{E}_{d,k}{}^{UN,EX} \tag{25}$$

$$\dot{C}_{d,k}{}^{AV,EN} = c_{f,k} \dot{E}_{d,k}{}^{AV,EN} \tag{26}$$

$$\dot{C}_{d,k}{}^{AV,EX} = c_{f,k} \dot{E}_{d,k}{}^{AV,EX} \tag{27}$$

$$\dot{Z}_k{}^{EX} = \dot{Z}_k - \dot{Z}_k{}^{EN} \tag{28}$$

$$\dot{Z}_k{}^{AV} = \dot{Z}_k - \dot{Z}_k{}^{UN} \tag{29}$$

$$\dot{Z}_k{}^{UN,EN} = \dot{E}_{p,k}{}^{EN} \left(\frac{\dot{Z}_k}{\dot{E}_{p,k}} \right)^{UN} \tag{30}$$

$$\dot{Z}_k{}^{UN,EX} = \dot{Z}_k{}^{UN} - \dot{Z}_k{}^{UN,EN} \tag{31}$$

$$\dot{Z}_k{}^{AV,EN} = \dot{Z}_k{}^{EN} - \dot{Z}_k{}^{UN,EN} \tag{32}$$

$$\dot{Z}_k{}^{AV,EX} = \dot{Z}_k{}^{EX} - \dot{Z}_k{}^{UN,X} \tag{33}$$

$$Em_{direct} = C(L_T(ALR)(EOL))(GWP + adp.GWP) \tag{34}$$

$$Em_{indirect} = Em_{energy} + Em_{eq.mfg} + Em_{eq.rcy} + Em_{re.mfg} \tag{35}$$

$$Em_{energy} = LT(AEC)EF \tag{36}$$

$$Em_{eq.mfg} = \sum MM(m) \tag{37}$$

Table 23
Performance evaluation results based on the conventional parameters.

Component	η_{ex}	$\eta_{ex,\mathrm{mod}}$	y_D	$y_D{}^{adv}$	f	$f^{AV,EN}$
ABScon	0.784	0.876	0.01261	0.03871	0.3067	0.005252
P1	0.1047	0.1952	0.05518	0.02663	0.5514	0.582
EV	0.9188	1	0.01173	$5.899x10^{-7}$	0.9915	1
ABS	0.4047	0.587	0.1432	0.07489	0.7764	0.042
SHX	0.9467	0.9893	0.2371	0.04534	0.4933	0.6144
P2	0.265	0.9922	0.0453	0.0001268	0.5254	0.983
Gen	0.493	0.8507	0.148	0.02527	0.1957	0.175
ORCT	0.9526	0.947	0.008493	0.03119	0.784	0.3273
ORCcon	0.7642	0.1905	0.002421	0.033	0.8473	0.01384
FPSC	0.01269	0.01203	0.2185	0.2246	0.6257	0.7621

Table 24
Performance evaluation results based on the developed novel indices.

Component, k	$\eta_{ex,EN,k}$	$\eta_{ex,EX,k}$	$\eta_{ex,UN,k}$	$\eta_{ex,AV,k}$	$ETIExPR,k$	$UNExFR,k$	$AVExFR,k$	$UNExPR,k$	$AVExPR$	UPI
Gen	0.555	0.321	0.658	0.241	0.207	0.853	0.284	1.139	0.139	0.711
ABScon	0.784	0.784	0.396	0.043	0.382	2.036	-	0.948	-	0.575
P1	0.105	0.105	0.822	0.670	0.403	1.626	1.838	12.772	11.772	0.962
EV	0.919	0.919	0.919	-	0.403	1.000	-	1	0.000	0.081
ABS	0.320	0.684	0.148	0.176	0.648	1.611	-	0.588	-	0.770
SHX	0.226	0.956	0.947	0.450	312.153	1.000	0	1	0	0.048
P2	0.265	0.265	0.000	1.372	87.857	0.663	-	0	-	0.867
V	0.968	1.134	0.975	-	0.044	1	0	1	-	0.015
ORCT	0.842	-	0.953	-	0.000	1.000	0	1	0.000	0.042
ORCcon	0.296	-	0.200	-	0.102	3.830	-	1	0.000	0.603
FPSC	0.012	-	0.267	-	0	0.048	0.953	1	0	1

$$Em_{eq.rcy} = \sum RM(mr) \tag{38}$$

$$Em_{re.mfg} = (C + (C(ALR)(LT)))RMF + C(1 - EOL)(RDF) \tag{39}$$

$$EEF_k = \frac{FExWR_k}{\eta_{ex,k}} \tag{40}$$

$$SEF_k = \frac{1}{1 - \eta_{ex,k}} \tag{41}$$

$$ExSI_k = \frac{1}{EEF_k} \tag{42}$$

$$SIIG = \frac{\dot{E}_{P,overall}}{\sum_{k=1}^{k=n} \dot{E}^{EN}{}_{F,k}} \tag{43}$$

$$SEIG = \frac{\dot{E}_{P,overall}}{\sum_{k=1}^{k=n} \dot{E}^{EX}{}_{F,k}} \tag{44}$$

$$\frac{1}{\eta_{ex,R}} = \frac{1}{SIIG} + \frac{1}{SEIG} \tag{45}$$

$$IExFR = \frac{\sum_{k=1}^{k=n} \dot{E}^{R}{}_{F,k}}{\sum_{k=1}^{k=n} \dot{E}^{EN}{}_{F,k}} \tag{46}$$

$$SIIG = \eta_{ex,R}(IExFR) \tag{47}$$

$$\eta_{ex,EN,k} = \frac{\dot{E}^{EN}{}_{P,k}}{\dot{E}^{EN}{}_{F,k}} \tag{48}$$

$$\eta_{ex,EX,k} = \frac{\dot{E}^{EX}{}_{P,k}}{\dot{E}^{EX}{}_{F,k}} \tag{49}$$

$$IMFR, k = \frac{\dot{M}^{EN,k}}{\dot{M}^{R,k}} \tag{50}$$

$$ETIExPR, k = \frac{\dot{E}^{EX}{}_{P,k}}{\dot{E}^{EN}{}_{P,k}} \tag{51}$$

$$\frac{1}{\eta_{ex,k,R}} = IMFR, k\left[\frac{1}{\eta_{ex,EN,k}} + \left(\frac{1}{\eta_{ex,EX,k}} ETIExPR, k\right)\right] \tag{52}$$

$$\eta_{ex,UN,k} = \frac{\dot{E}^{UN}{}_{P,k}}{\dot{E}^{UN}{}_{F,k}} \tag{53}$$

$$\eta_{ex,AV,k} = \frac{\dot{E}^{AV}{}_{P,k}}{\dot{E}^{AV}{}_{F,k}} \tag{54}$$

$$UNExFR, k = \frac{\dot{E}^{UN}{}_{F,k}}{\dot{E}^{R}{}_{F,k}} \tag{55}$$

$$AVExFR, k = \frac{\dot{E}^{AV}{}_{F,k}}{\dot{E}^{R}{}_{F,k}} \tag{56}$$

$$AVExPR = \frac{\dot{E}^{AV}{}_{P,k}}{\dot{E}^{R}{}_{P,k}} \tag{57}$$

$$UNExPR = \frac{\dot{E}^{UN}{}_{P,k}}{\dot{E}^{R}{}_{P,k}} \tag{58}$$

$$\eta_{ex,UN,k} = \eta_{ex,R}\left(\frac{1}{UNExFR, k}\right)(UNExPR) \tag{59}$$

$$\eta_{ex,AV,k} = \eta_{ex,R}\left(\frac{1}{AVExFR, k}\right)(AVExPR) \tag{60}$$

$$UPI_{,k} = \frac{(1 - \eta_{ex,R}) - \left[\left(\frac{1}{UNExPR,k}\right) UNExFR, k - \left((UNExPR, k)\eta_{ex,R}\right)\right]}{\left[\left(\frac{1}{UNExPR,k}\right) UNExFR, k - \left((UNExPR, k)\eta_{ex,R}\right)\right]} \tag{61}$$

$$\dot{E}^{R}{}_{P,total} = \dot{E}^{EN}{}_{P,total} + \dot{E}^{EX}{}_{P,total} \tag{62}$$

$$\sum_{k=1}^{k=n} \dot{E}^{R}{}_{F,k} = \sum_{k=1}^{k=n} \dot{E}^{EN}{}_{F,k} + \sum_{k=1}^{k=n} \dot{E}^{EX}{}_{F,k} \tag{63}$$

$$\frac{\dot{E}^{EN}{}_{P,k}}{\dot{E}^{R}{}_{P,k}} = \frac{\dot{M}^{EN,k}}{\dot{M}^{R,k}} \tag{64}$$

$$\dot{E}^{UN}{}_{D,k} = \dot{E}^{R}{}_{P,k}\left(\frac{\dot{E}_{D,k}}{\dot{E}_{P,k}}\right)^{UN} \tag{65}$$

Financial funding and support

This research did not receive any specific grant from funding agencies in the public, commercial, or not-for-profit sectors.

CRediT authorship contribution statement

All the authors were involved in the preparation of the manuscript while their contributions are listed below. **Aslı Tiktaş:** Conceptualization, Methodology, Investigation, Formal analysis, Drawing the pictures, Writing & editing. **Huseyin Gunerhan:** Conceptualization, Methodology, Supervision, Writing – review & editing. **Arif Hepbasli:** Conceptualization, Methodology, Supervision, Writing – review & editing. **Emin Açıkkalp:** Conceptualization, Methodology, Supervision, Writing – review & editing.

Declaration of Competing Interest

The authors declare that they have no known competing financial interests or personal relationships that could have appeared to influence the work reported in this paper.

Acknowledgments

The authors are very grateful to the reviewers and editor for their valuable and constructive comments, which led to increasing the quality of the paper.

References

Alsagri, A.S., Arabkoohsar, A., Alrobaian, A.A., 2019. Combination of subcooled compressed air energy storage system with an Organic Rankine Cycle for better electricity efficiency, a thermodynamic analysis (Dec.). J. Clean. Prod. vol. 239. https://doi.org/10.1016/j.jclepro.2019.118119.

Azizi, S., Shakibi, H., Shokri, A., Chitsaz, A., Yari, M., 2023. Multi-aspect analysis and RSM-based optimization of a novel dual-source electricity and cooling cogeneration system (Feb.). Appl. Energy vol. 332. https://doi.org/10.1016/j.apenergy.2022.120487.

Bagherzadeh, S.A., Ruhani, B., Namar, M.M., Alamian, R., Rostami, S., 2020. Compression ratio energy and exergy analysis of a developed Brayton-based power cycle employing CAES and ORC. J. Therm. Anal. Calorim. vol. 139 (4), 2781–2790. https://doi.org/10.1007/s10973-019-09051-5.

Balli, O., Caliskan, H., 2021. On-design and off-design operation performance assessmentsof an aero turboprop engine used on unmanned aerial vehicles (UAVs) in terms of aviation, thermodynamic, environmental and sustainability perspectives. Energy Convers. Manag. vol. 243 (June), 0–1. https://doi.org/10.1016/j.enconman.2021.114403.

Concentrating Solar Power Projects _ NREL.

Bet Sarkis, R., Zare, V., 2018. Proposal and analysis of two novel integrated configurations for hybrid solar-biomass power generation systems: thermodynamic and economic evaluation (no. January). Energy Convers. Manag. vol. 160, 411–425. https://doi.org/10.1016/j.enconman.2018.01.061.

bp, Statistical Review of World Energy 2022.

Chaiyat, N., 2014. Upgrading of low temperature heat with absorption heat transformer for generating electricity by organic rankine cycle. Glob. Adv. Res. J. Eng., Technol. Innov. vol. 3 (9), 235–247.

D. Chuquin-Vasco, C. Calderón-Tapia, N. Chuquin-Vasco, J. Chuquin-Vasco, D. Aguirre-Ruiz, and D.V. Ch, © ICAS 2023 Modeling a Binary Organic Rankine Cycle Operated With Solar Collectors: Case Study-Ecuador, 2023. [Online]. Available: www.e-afr.orgwww.e-afr.org.

Díaz Carrillo, J.J., 2023. Solar thermal cooling systems driven by linear Fresnel collectors, realistic and practical simulation tool, cases studies applications and machine learning as a control approach. E. T. S. I. Ind. (UPM).

Donnellan, P., Byrne, E., Oliveira, J., Cronin, K., 2014. First and second law multidimensional analysis of a triple absorption heat transformer (TAHT). Appl. Energy vol. 113, 141–151. https://doi.org/10.1016/j.apenergy.2013.06.049.

Emadi, M.A., Chitgar, N., Oyewunmi, O.A., Markides, C.N., 2020. Working-fluid selection and thermoeconomic optimisation of a combined cycle cogeneration dual-loop organic Rankine cycle (ORC) system for solid oxide fuel cell (SOFC) waste-heat recovery (Mar.). Appl. Energy vol. 261. https://doi.org/10.1016/j.apenergy.2019.114384.

Horuz, I., Kurt, B., 2010. Absorption heat transformers and an industrial application. Renew. Energy vol. 35 (10), 2175–2181. https://doi.org/10.1016/j.renene.2010.02.025.

Javed, S., Tiwari, A.K., 2023. Performance assessment of different Organic Rankine Cycle (ORC) configurations driven by solar energy (no. January). Process Saf. Environ. Prot. vol. 171, 655–666. https://doi.org/10.1016/j.psep.2023.01.039.

Jie Ling, J.L., Go, E.S., Park, Y.K., Lee, S.H., 2022. Recent advances of hybrid solar - biomass thermo-chemical conversion systems. no. September 2021 Chemosphere vol. 290, 133245. https://doi.org/10.1016/j.chemosphere.2021.133245.

Karabuga, A., Yakut, M.Z., Utlu, Z., 2023. Assessment of thermodynamic performance of a novelty solar-ORC configuration based hydrogen production: an experimental study. Int J. Hydrog. Energy. https://doi.org/10.1016/j.ijhydene.2023.05.093.

Kumar, M., 2023. A review study on organic rankine cycles coupled with latent thermal energy storage systems using solar energy as heat source. Int. J. Adv. Eng. Manag. (IJAEM) vol. 5, 521. https://doi.org/10.35629/5252-0501521534.

Li, Q., et al., 2023. Simulation study on solar single/double-effect switching LiBr-H2O absorption refrigeration system (Apr.). Energy vol. 16 (7). https://doi.org/10.3390/en16073220.

Liu, F., Sui, J., Liu, T., Jin, H., 2017. Energy and exergy analysis in typical days of a steam generation system with gas boiler hybrid solar-assisted absorption heat transformer. Appl. Therm. Eng. vol. 115, 715–725. https://doi.org/10.1016/j.applthermaleng.2017.01.011.

Liu, Z., Xie, N., Yang, S., 2020. Thermodynamic and parametric analysis of a coupled LiBr/H2O absorption chiller/Kalina cycle for cascade utilization of low-grade waste heat (Feb.). Energy Convers. Manag vol. 205. https://doi.org/10.1016/j.enconman.2019.112370.

Ma, L., Zhao, Q., Guo, X., Zhang, H., Hu, Z., Hou, S., 2021. A hybrid system consisting of dye-sensitized solar cell and absorption heat transformer for electricity production and heat upgrading. Process Saf. Environ. Prot. vol. 150, 233–241. https://doi.org/10.1016/j.psep.2021.04.013.

Machado, D.O., et al., 2023. Digital twin of a Fresnel solar collector for solar cooling (Jun.). Appl. Energy vol. 339. https://doi.org/10.1016/j.apenergy.2023.120944.

Mohammadi, A., Kasaeian, A., Pourfayaz, F., Ahmadi, M.H., 2017. Thermodynamic analysis of a combined gas turbine, ORC cycle and absorption refrigeration for a CCHP system (Jan.). Appl. Therm. Eng. vol. 111, 397–406. https://doi.org/10.1016/j.applthermaleng.2016.09.098.

Mosaffa, A.H., Farshi, L.G., 2020. Novel post combustion CO_2 capture in the coal-fired power plant employing a transcritical CO_2 power generation and low temperature steam upgraded by an absorption heat transformer. no. November 2019 Energy Convers. Manag. vol. 207, 112542. https://doi.org/10.1016/j.enconman.2020.112542.

Navongxay, B., Chaiyat, N., 2019. Energy and exergy costings of organic Rankine cycle integrated with absorption system (Apr.). Appl. Therm. Eng. vol. 152, 67–78. https://doi.org/10.1016/j.applthermaleng.2019.02.018.

Nikbakhti, R., Wang, X., Hussein, A.K., Iranmanesh, A., 2020. Absorption cooling systems – review of various techniques for energy performance enhancement. Mar. 01. In: Alexandria Engineering Journal, vol. 59. Elsevier B.V.,, pp. 707–738. https://doi.org/10.1016/j.aej.2020.01.036.

P. Hwang, Y., Ferreira, C. I., Guideline for life cycle climate performance, 2015.

Permana, D.I., Rusirawan, D., Farkas, I., 2022. A bibliometric analysis of the application of solar energy to the organic Rankine cycle. Heliyon vol. 8 (4), e09220. https://doi.org/10.1016/j.heliyon.2022.e09220.

Pop, O.G., et al., 2023. Analytical modelling of food storage cooling with solar ammonia-water absorption system, powered by parabolic trough collectors. Method (Jan.). MethodsX vol. 10. https://doi.org/10.1016/j.mex.2023.102013.

Quoilin, S., Broek, M.Van Den, Declaye, S., Dewallef, P., Lemort, V., 2013. Techno-economic survey of organic rankine cycle (ORC) systems. Renew. Sustain. Energy Rev. vol. 22, 168–186. https://doi.org/10.1016/j.rser.2013.01.028.

Razmi, A., Soltani, M., Torabi, M., 2019. Investigation of an efficient and environmentally-friendly CCHP system based on CAES, ORC and compression-absorption refrigeration cycle: energy and exergy analysis (Sep.). Energy Convers. Manag vol. 195, 1199–1211. https://doi.org/10.1016/j.enconman.2019.05.065.

Sigue, S., Abderafi, S., Vaudreuil, S., Bounahmidi, T., 2023. Design and steady-state simulation of a CSP-ORC power plant using an open-source co-simulation framework combining SAM and DWSIM (Jan.). Therm. Sci. Eng. Prog. vol. 37. https://doi.org/10.1016/j.tsep.2022.101580.

Smith, R., 2005. Chem. Process Des. Integr.

Tiktas, A., Gunerhan, H., Hepbasli, A., 2022. Single and multigeneration Rankine cycles with aspects of thermodynamical modeling, energy and exergy analyses and optimization: a key review along with novel system description figures (no. February). Energy Convers. Manag.: X vol. 14, 100199. https://doi.org/10.1016/j.ecmx.2022.100199.

Wakim, M., Rivera-Tinoco, R., 2019. Absorption heat transformers: sensitivity study to answer existing discrepancies. Renew. Energy vol. 130, 881–890. https://doi.org/10.1016/j.renene.2018.06.111.

Wang, D., Li, S., Liu, F., Gao, L., Sui, J., 2018a. Post combustion CO_2 capture in power plant using low temperature steam upgraded by double absorption heat transformer. no. May 2017 Appl. Energy vol. 227, 603–612. https://doi.org/10.1016/j.apenergy.2017.08.009.

Wang, J., Han, Z., Liu, Y., Zhang, X., Cui, Z., 2021. Thermodynamic analysis of a combined cooling, heating, and power system integrated with full-spectrum hybrid solar energy device (no. July). Energy Convers. Manag. vol. 228, 113596. https://doi.org/10.1016/j.enconman.2020.113596.

Wang, M., Wang, Y., Feng, X., Deng, C., Lan, X., 2018b. Energy performance comparison between power and absorption refrigeration cycles for low grade waste heat recovery (Apr.). ACS Sustain Chem. Eng. vol. 6 (4), 4614–4624. https://doi.org/10.1021/acssuschemeng.7b03589.

Xu, A., et al., 2021. Performance analysis of a cascade lithium bromide absorption refrigeration/dehumidification process driven by low-grade waste heat for hot summer and cold winter climate area in China (Jan.). Energy Convers. Manag vol. 228. https://doi.org/10.1016/j.enconman.2020.113664.

Yağlı, H., Koç, Y., Kalay, H., 2021. Optimisation and exergy analysis of an organic Rankine cycle (ORC) used as a bottoming cycle in a cogeneration system producing steam and power. no. May 2020 Sustain. Energy Technol. Assess. vol. 44. https://doi.org/10.1016/j.seta.2020.100985.

Yang, S., Deng, C., Liu, Z., 2019. Optimal design and analysis of a cascade LiBr/H_2O absorption refrigeration/transcritical CO_2 process for low-grade waste heat recovery (Jul.). Energy Convers. Manag vol. 192, 232–242. https://doi.org/10.1016/j.enconman.2019.04.045.

Yari, M., Salehi, S., Mahmoudi, S.M.S., 2017. Three-objective optimization of water desalination systems based on the double-stage absorption heat transformers. Desalination vol. 405, 10–28. https://doi.org/10.1016/j.desal.2016.12.001.

Zhou, T., Liu, J., Ren, J., Yang, S., 2021. Comprehensive assessment of a coupled LiBr/H2O absorption refrigeration/ORC system for low-grade residual heat recovery based on advanced exergy and exergoeconomic analysis. ACS Sustain Chem. Eng. https://doi.org/10.1021/acssuschemeng.1c08611.